Engineering 5 (2019) 702–720

Contents lists available at ScienceDirect

Engineering

journal homepage: www.elsevier.com/locate/eng

Research
Additive Manufacturing—Review

Development of Micro Selective Laser Melting: The State of the Art and Future Perspectives

Balasubramanian Nagarajan, Zhiheng Hu, Xu Song, Wei Zhai, Jun Wei *

*Singapore Institute of Manufacturing Technology (SIMTech), Agency for Science, Technology and Research (A*STAR), Singapore 637662, Singapore*

ARTICLE INFO

Article history:
Received 27 July 2018
Revised 31 January 2019
Accepted 14 March 2019
Available online 3 July 2019

Keywords:
Additive manufacturing
Selective laser melting
Microfabrication
Hybrid processing
Powder-bed recoating

ABSTRACT

Additive manufacturing (AM) is gaining traction in the manufacturing industry for the fabrication of components with complex geometries using a variety of materials. Selective laser melting (SLM) is a common AM technique that is based on powder-bed fusion (PBF) to process metals; however, it is currently focused only on the fabrication of macroscale and mesoscale components. This paper reviews the state of the art of the SLM of metallic materials at the microscale level. In comparison with the direct writing techniques that are commonly used for micro AM, micro SLM is attractive due to a number of factors, including a faster cycle time, process simplicity, and material versatility. A comprehensive evaluation of various research works and commercial systems for the fabrication of microscale parts using SLM and selective laser sintering (SLS) is conducted. In addition to identifying existing issues with SLM at the microscale, which include powder recoating, laser optics, and powder particle size, this paper details potential future directions. A detailed review of existing recoating methods in powder-bed techniques is conducted, along with a description of emerging efforts to implement dry powder dispensing methods in the AM domain. A number of secondary finishing techniques for AM components are reviewed, with a focus on implementation for microscale features and integration with micro SLM systems.

1. Introduction

In recent times, there has been an ever-increasing demand for microfabrication technologies to cater to the drive toward miniaturization that is occurring in several sectors, including the electronics, medical, automotive, biotechnology, energy, communications, and optics [1]. Numerous products and components, including micro-actuators, micro-mechanical devices, sensors and probes, microfluidic components, medical implants, microswitches, optical devices, memory chips, micro-motors, magnetic hard drive heads, computer processors, inkjet printing heads, lead frames, electrical connectors, micro fuel cells and, most importantly, micro-electromechanical systems (MEMS) devices, are made by means of microfabrication techniques. Microscale manufacturing processes are generally classified into MEMS-based (or lithography-based) and non-MEMS-based (or non-lithography-based) processes. The utilization of metallic materials in microcomponents has gained momentum, largely due to the applicability resulting from their mechanical and electrical properties (i.e., strength, ductility, electrical conductivity, etc.) [2]. The processing of metals in microfabrication is commonly achieved through non-lithography-based techniques such as machining, forming, and joining [3]. Traditional micromanufacturing methods have one or more of the following limitations: difficulty in fabricating complex shapes, material limitations, tooling-related issues, inability to perform real three-dimensional (3D) fabrication, and so forth.

The development of additive manufacturing (AM) technology over the past two decades has opened up new horizons in metal fabrication, given the ability of AM to realize any complex geometry [4,5]. AM consolidates powder or wire feedstock into a final product in a layer-by-layer manner. AM processes start with 3D modeling of the desired component, which is then sliced into different two-dimensional (2D) layers. The feedstock is then deposited, followed by the selective addition of every layer using an energy source [6]. AM techniques are commonly classified into seven categories: material extrusion, vat photopolymerization, material jetting, binder jetting, sheet lamination, directed energy deposition (DED), and powder-bed fusion (PBF) [7]. Material extrusion, vat photopolymerization, and material jetting are generally

* Corresponding author.
E-mail address: jwei@SIMTech.a-star.edu.sg (J. Wei).

https://doi.org/10.1016/j.eng.2019.07.002

used for non-metallic materials. Sheet lamination is capable of processing metals, based on the precision slicing of metal sheets with subsequent stacking using bonding, welding, or ultrasonic consolidation [8]. However, binder jetting, DED, and PBF have been identified as the most suitable processes to process metals [6,7,9]. Binder jetting works by depositing binder adhesive on metal powder, followed by curing to form a "green" part [10]. The final part is achieved by sintering the green part with an optional infiltration of another material or of nanoparticles of the same metal. Mandatory heat treatment and high porosity are the common limitations of the binder jet process, as they hinder its ability to be applicable at the microscale [11]. DED—which is also known as laser cladding, laser metal deposition (LMD), and laser-engineered net spacing (LENS)—is another significant AM process used to fabricate metal components [12]. In DED, the feedstock is directly deposited into the melt pool, which is created by a focused energy source. The feedstock can either be powder or wire, where powder-fed DED typically has better resolution than wire-fed DED [7]. Since DED produces only near-net shapes, further post-processing is necessary. PBF is typically preferred for manufacturing small components that require a good surface finish, as PBF demonstrates better resolution than DED [4]. PBF generally has a smaller melt pool and layer thickness, resulting in better resolution and surface finish. PBF processes involve the selective melting or sintering of a layer of powder using an energy source. Electron beam and laser beam are the two main energy sources used in PBF processes—that is, in electron beam melting (EBM) and in selective laser melting (SLM)/selective laser sintering (SLS), respectively. In addition, SLM is capable to produce components with mechanical properties that are comparable to that of the traditional manufacturing processes [13].

Even though metallic AM has already been commercialized for various applications in the biomedical and aerospace sectors, including the production and repair of aerospace components [5], the application of AM has been limited to macroscale and mesoscale fabrication. AM techniques for microscale fabrication are only recently being developed for the production of 3D microfeatures on a variety of materials including ceramics, polymers, and metals [14]. The following section focuses on past AM approaches for fabricating metallic microcomponents.

2. Micro metallic AM

AM at the microscale and nanoscale has attracted attention in recent years, as is evident from the emergence of review papers of corresponding techniques [14–16]. Engstrom et al. [15] published a review of additive nanomanufacturing (ANM) techniques that produce final parts with a resolution of sub-100 nm using various materials including metals, polymers, and organic molecules. The review by Hirt et al. [16] focused exclusively on micro AM techniques for metals, which are classified into metal transfer and *in situ* synthesis techniques. By definition, the benchmark feature size for micro AM techniques is described as 10 μm. Vaezi et al. [14] classified 3D micro AM techniques into two main categories—namely, 3D direct writing and scalable AM—as illustrated in Fig. 1. 3D direct writing is comprised of ink-based nozzle dispensing and aerosol jet techniques, laser transfer techniques, and beam deposition methods such as laser chemical vapor deposition (LCVD), focused ion beam (FIB) writing, and electron beam (EB) writing. Although the direct writing process typically has a high resolution that is suitable for nanoscale fabrication, the processing has been highly complex and slow [15,16]. In the category of scalable AM techniques, micro-stereolithography (MSL) has been the most successful micro AM technique due to its high resolution and repeatability, although it is limited by the choice of materials [17]. Fused deposition modeling (FDM) and laminated object manufacturing (LOM) techniques have difficulties in processing metals, besides their limitation to achieve high feature resolution. While metal inks have been used in inkjet printing [18], this method is still strongly restricted to non-metals. 3D printing (3DP)/binder jet printing (BJP) shows promise in terms of multimaterial printing and cold processing, but the printed parts typically have high porosity [19].

For processing metals without any resins (as in MSL) or binders (as in 3DP or BJP), SLM and SLS—that is, powder-bed-based layer-by-layer melting or sintering using lasers—have demonstrated potential due to their ability to fabricate true 3D microparts with high resolution [14,20]. The vast amount of available knowledge on the use of SLM and SLS in macroscale processing could be used to scale down the technique to the microscale. This review focuses exclusively on SLM and SLS for the fabrication of microscale features. The difference between SLM and SLS lies in the degree of melting [6]. SLM achieves complete melting of the powder, whereas SLS only sinters—or partially melts—the powder. With the exception of the full or partial melting of powder particles, there is no difference between SLM and SLS in terms of process setup and mechanisms. Therefore, in this paper, SLM and SLS are considered to be identical for the purpose of comparing process components and parameters. The discussion on the powder-recoating system and hybrid processing in the later sections can also be applied to the miniaturization of other PBF techniques.

3. Selective laser melting

Fig. 2 shows a schematic of the SLM process setup. In SLM and SLS, a layer of powder is first spread on the build substrate. The laser beam melts or sinters the powder according to the required geometry. The recoater then applies the next layer of powder over the solidified part, followed by further laser melting/sintering. The heating and cooling rates are very high during the SLM process due to the short interaction time between the laser source and the powder. Since the resultant melt pool geometry significantly influences the microstructure features, the mechanical properties of the fabricated part differ from those of conventional processes [13]. Detailed reviews of the process mechanisms during SLM can be

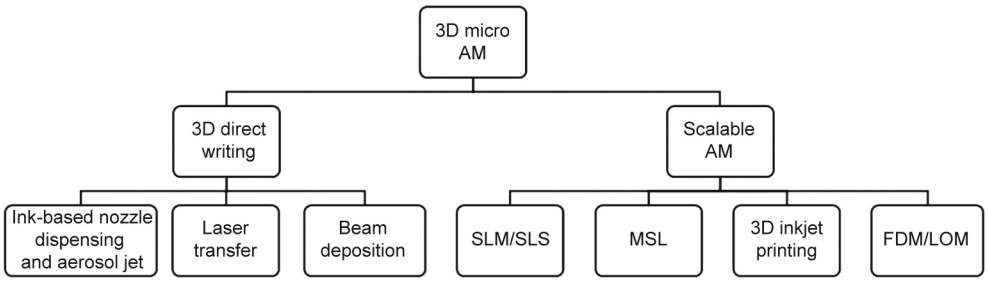

Fig. 1. Major classification of AM techniques for microscale fabrication. MSL: micro-stereolithography; FDM: fused deposition modeling; LOM: laminated object manufacturing. Reproduced from Ref. [14] with permission of Springer-Verlag London, © 2012.

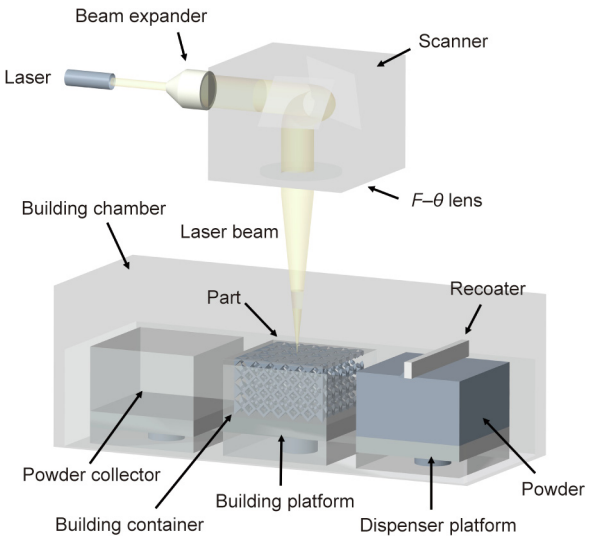

Fig. 2. Schematic of the SLM process.

found elsewhere, in Refs. [6,7,21]. The final quality of the SLM parts is influenced by a large number of process parameters due to the complex system and mechanisms involved [22–29].

The SLM process parameters can be classified roughly into powder-related, laser-related, and powder-bed-related variables according to the properties, as illustrated in Fig. 3. Most of the powder-related process parameters, such as the chemical composition, size and shape of the particles, and surface morphology, are invariants in an actual production environment [7]. The parameters related to laser systems that influence the SLM process include the laser type (i.e., continuous wave (CW) or pulsed), laser power, and spot size. The scanning parameters—such as scanning strategy, hatch spacing, and scanning speed—significantly affect the SLM built part characteristics [30]. The third classification of SLM process parameters is powder-bed characteristics. In most powder-bed processes, the powder is applied onto the building platform by means of a raking mechanism, which is also known as recoating. The efficiency of the powder delivery system is influenced by a number of parameters, including the recoater type, number of recoating passes, amount of retrieved powder during each pass and—most importantly—powder properties. The thickness of the recoating layer is one of the significant process parameters that control the part properties. Layer thickness, particle size distribution (PSD), and laser parameters influence the laser–material interaction and hence the melt pool characteristics.

The characteristics of AM components made using SLM are typically evaluated through a number of process outcomes, depending on the application. Fig. 4 summarizes some of the important features of SLM-fabricated parts. As in any conventional process, the feature resolution, surface finish, mechanical properties, and microstructure are characterized in order to evaluate the quality of the final built part and thereby the SLM process. Fig. 5 illustrates the different possible defects that may occur in SLM. The formation of defects is essentially dependent on the process variables, which need to be optimized in order to fabricate defect-free components. A detailed review of the defects in AM processes is available elsewhere [7].

4. Micro selective laser melting

Commercial SLM systems generally employ powder particle sizes of 20–50 μm and a layer thickness ranging from 20 to 100 μm. The effort to scale down conventional SLM in order to increase the feature resolution involves three main factors: laser beam diameter, layer thickness, and particle size, as illustrated in Fig. 6. Fischer et al. [31] defined the scale of micro SLM to be the following: a laser beam diameter < 40 μm, a layer thickness < 10 μm, and a particle size < 10 μm.

4.1. Current state of the art

The first micro SLS system—known as laser micro sintering—was developed more than a decade ago at the Laserinstitut Mittelsachsen e.V. [32] using a Q-switched neodymium-doped yttrium aluminum garnet (Nd:YAG) laser (0.5 to 2 kW). This system involves a special raking procedure that applies a thick layer of powder first, which is successively sheared off from opposite directions to produce a thin layer. The drives for the powder dispenser and building platform have a resolution of 0.1 μm in order to control the layer thickness with sub-micrometer accuracy. With this first approach, the microparts that were fabricated had a structural resolution of less than 30 μm and an aspect ratio greater than 10, with a surface roughness of 5 μm. Various metals including tungsten (W), aluminum (Al), copper (Cu), and silver (Ag), with an average powder particle size ranging from 0.3 to 10 μm, were tested for this study, as shown in Fig. 7 [20,33,34]. Fig. 7(a) [33] shows one of the initial features built by this setup using 300 nm tungsten powder. Although the exposure of the powder to a vacuum of 10^{-3} Pa produced better raking, the powder-bed density (PBD) after raking was still around 15%. A maximum part density of 90% after sintering was observed with a W and Cu powder mixture.

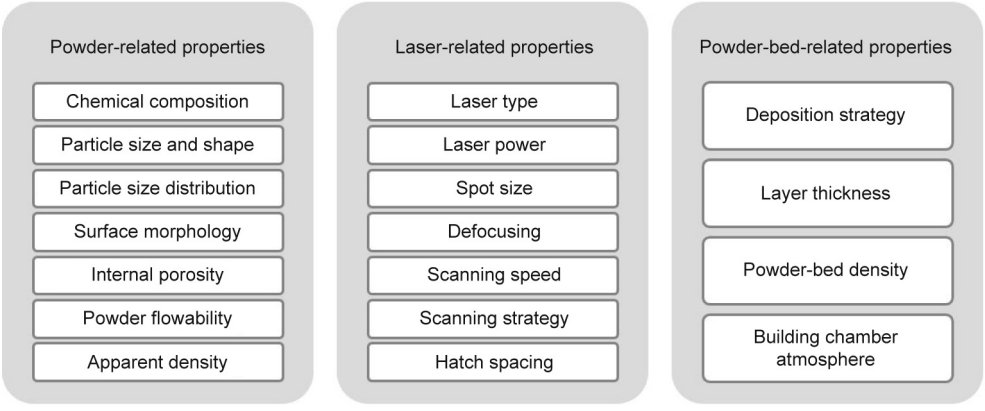

Fig. 3. Summary of SLM process parameters.

The same research group has developed an improved system involving two rakes with a circular cross-section to spread the powder [20,35]. Figs. 7(b)–(d) [20,33,34] show the different feature shapes that have been fabricated with this modified setup. The difference lies in the powder-recoating mechanism, as the rakes traverse in a circular motion between the powder reservoir and the building platform. Metal cylinders with a sharpened edge are used as the rake blade. This design with two or more rakes facilitates built parts with multiple materials or a grain size gradient along the part thickness, as shown in Fig. 7(d). In addition to raking, the recoating system can be used to manually compact the powder by pressure. With this unique setup, microparts of various metals including tungsten, aluminum, copper, silver, 316L, molybdenum (Mo), titanium (Ti), and 80Ni20Cr can be produced using laser micro sintering. After continuous improvement of the process characteristics, the laser micro sintering of metals has yielded a minimum resolution of 15 μm and a surface roughness of 1.5 μm. A maximum part density of 98% and 95% was reported for oxide ceramics and alloys, respectively [36].

Gieseke et al. [37,38] developed a micro SLM system in 2013 to produce American Iron and Steel Institute (AISI) 316L hollow microneedles with a minimum wall thickness of 50 μm. The laser spot diameter was scaled down to 19.4 μm in order to achieve fine features. A particle size ranging from 5 to 25 μm was used to build needles with an inner diameter of 160 μm using a layer thickness of 20 μm. Despite the combination of fine spot size and finer powders, the surface roughness of the built parts was poor ($R_a \approx 8$ μm). Agglomeration of fine powder could have resulted in non-uniform powder spreading, which would explain the poor finish. A significant powder adherence occurred along the wall due to the high energy input. More complex helix shapes with a minimum strut diameter of 60 μm were also produced, albeit with the occurrence of partial strut failure [38]. The same research group [39] fabricated parts using shape memory alloys (Ni–Ti), as shown in Fig. 8(a), with a resolution of 50 μm at a lower laser power and higher scanning speed. Yadroitsev and Bertrand [40] used a commercial system, PM 100, to fabricate microfluidic systems made of stainless steel (SS) 904L, as shown in Fig. 8(b). The spot size

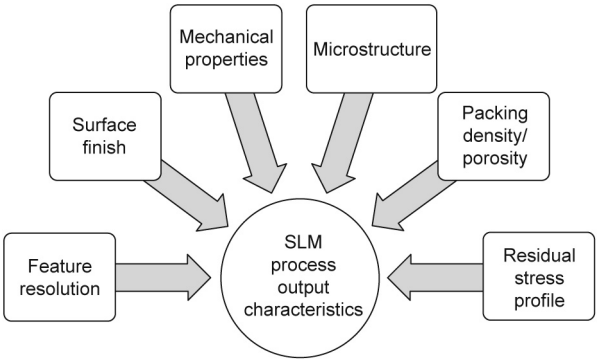

Fig. 4. Summary of SLM process output characteristics.

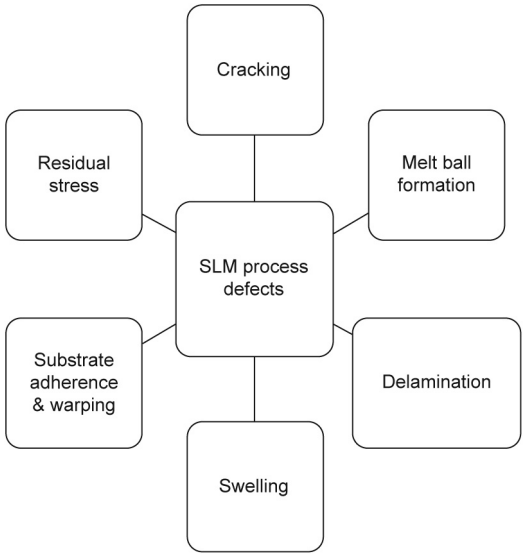

Fig. 5. Typical SLM process defects.

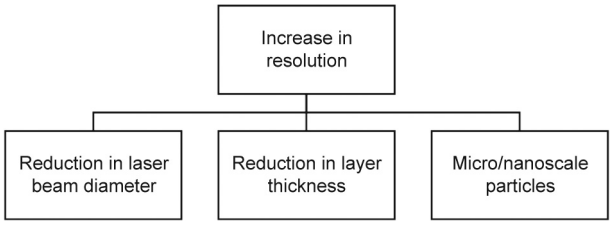

Fig. 6. Requirements for the SLM of microscale features.

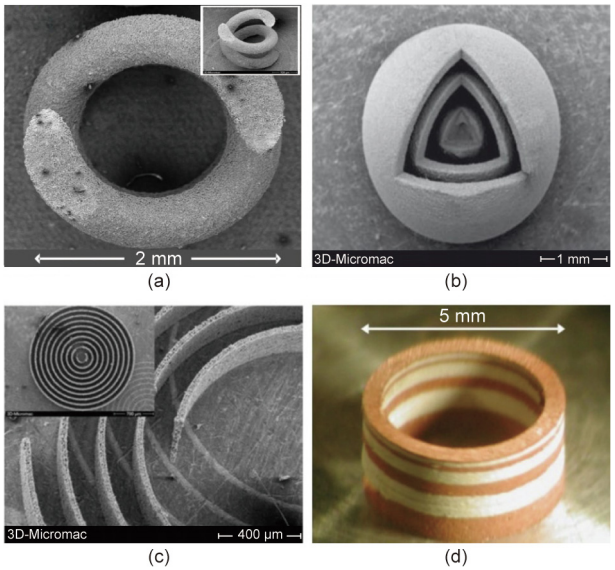

Fig. 7. Fabrication of microfeatures by laser micro sintering. (a) Sintered test structures made of tungsten powder (300 nm size); (b) three nested hollow spheres; (c) concentric rings; (d) laser sintering of multi-materials (Cu and Ag). (a) and (d) are reproduced from Ref. [33] with permission of Emerald Group Publishing Limited, © 2007; (b) is reproduced from Ref. [20] with permission of WILEY-VCH Verlag GmbH & Co. KGaA, © 2007; (c) is reproduced from Ref. [34] with permission of Emerald Group Publishing Limited, © 2005.

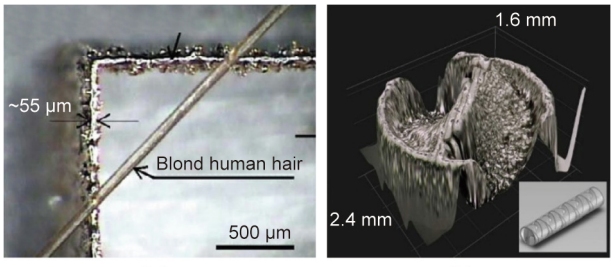

Fig. 8. Parts fabricated using micro SLM. (a) Ni–Ti micro actuators; (b) top view of SS 904L microfluidic systems, the insert image is its internal structure. (a) is reproduced from Ref. [39] with permission of Elsevier B.V., © 2010; (b) is reproduced from Ref. [40] with permission of DAAAM International, © 2010.

and layer thickness were 70 and 5 μm, respectively. Fully functional parts of 100–500 μm with structural elements of 20 μm were produced. It is worth noting that the spot size was still large and the surface roughness was poor.

In 2014, Fischer et al. [31] investigated the process parameters of micro SLM using an EOSINT μ60 system. The minimum roughness and the maximum feature resolution achieved were 7.3 and 57 μm, respectively. A maximum relative density of 99.32% was attained for the SLM of cuboidal structures. Despite a relatively finer powder of 3.5 μm, the achieved resolution is not sufficient for the dimensional specifications of microcomponents. Abele and Kniepkamp [41] further improved the surface quality of the parts fabricated by micro SLM by using the contour-scanning strategy. A minimum surface roughness of 1.69 μm was achieved along the walls parallel to the building direction. Kniepkamp et al. [42] also reported on the fabrication of micro SLM parts with a top surface roughness of less than 1 μm, using parametric optimization. Very recently, Roberts and Tien [43] reported on the fabrication of SS microelectrode arrays using micro SLS with a vertical and lateral resolution of 5 and 30 μm, respectively.

The latest effort in micro AM is from the University of Texas at Austin [44,45], where a micro SLS system composed of an ultrafast laser, a micro-mirror-based optical system, substrate heating, and a precise recoating system has been developed to achieve a feature resolution of 1 μm. Three significant modifications to typical SLS systems have been performed:

- A new spreader design has been incorporated, which includes a combination of a precision blade and a precision roller. The roller is attached with a linear voice coil actuator to provide very low amplitude high-frequency vibration. With the new setup, vibration compaction is included to achieve fine layers of a few micrometers.
- The galvanometric mirrors commonly used in SLM machines have been replaced with digital micro-mirror devices (DMDs) in this system to increase the system throughput.
- Additional focusing optics have been added to achieve a spot size of 1 μm. In addition, a linear actuating system for displacing the powder bed with a resolution of a few tens of nanometers has been implemented.

Despite the inclusion of a vibrating roller as the powder spreader in the SLS system [45], agglomeration of the powder particles was still observed. Two modifications to the micro SLS system have been implemented: ① replacing dry powder with nanoparticle inks, and ② changing the particle-dispensing mechanism from traditional blade/rollers to slot die- or spin-coating techniques. In the improved setup, the micro SLS design was changed to include a slot die-coating mechanism, due to its flexibility. Slot die coating is capable of depositing a wide range of thicknesses ranging from 20 nm to 150 μm through precise metering and controlled dispensing [44]. In addition, a precise nanopositioning stage using voice coil actuators was used to achieve fine precision. However, this system was only applicable for slurries or inks, due to nanoparticle agglomeration of the fine dry powder caused by van der Waals forces [46].

Table 1 [31,32,35,37,38,42,43] summarizes the research works that have been carried out on the use of micro SLM/SLS to process metallic materials. It is worth noting that both CW and pulsed lasers are being used in micro SLM systems, which is different from the prominent use of CW lasers in conventional SLM systems. Regenfuss et al. [33] initially used a Q-switched pulsed laser for a laser micro sintering setup. The Q-switched laser was shown to be effective for the following reasons: ① an increase in part resolution; ② a reduction in residual stress; ③ a reduction in oxidation effect, possibly due to gas or plasma expansion, which provided a shielding effect; ④ the elimination of issues such as poor substrate–part adherence and material sublimation at low pressure, which typically occur with the sintering of sub-micrometer powders using a CW laser; and ⑤ suitability to process dielectrics. The pulsed lasers produced narrow and deep cut-ins, frozen jets, and flattened craters due to a higher laser intensity in comparison with the CW lasers. However, the pulsed laser resulted in a poor surface finish, irregular tracks, and balling, due to an unstable melt pool. Ke et al. [47] compared CW and pulsed laser modes in the laser micro sintering of fine nickel (Ni) powder with a mean particle size of 4 μm. It was reported that the CW laser resulted in a more pronounced balling phenomenon than the pulsed laser; use of the latter reduced the balling due to the flattening effect by the plasma and the rapid cooling rate. Moreover, the pulsed laser was observed to result in a better wettability. However, the single tracks produced by the pulsed laser had corrugation, trench formation, and poor surface finish. Similarly, Kniepkamp et al. [42] reported on the poor surface finish and discontinuous tracks that occurred when using the pulsed mode of a 50 W fiber laser. Fischer et al. [31] observed that the pulsed laser could not produce homogenous single tracks without defects, despite testing a wide range of laser powers and pulse repetition rates. In addition to its use with metals, a pulsed wave laser in micro SLS has been tested with ceramics and was found to be effective [48].

Table 1
Literature review of SLM/SLS techniques for microscale fabrication.

Specifications	Regenfuss et al. [32]	Streek et al. [35]	Gieseke et al. [37,38]	Fischer et al. [31,42]	Roberts and Tien [43]
Structural resolution (μm)	< 30	15	< 50	< 40	30
Aspect ratio	> 10	NS	30:1	262	NS
Layer thickness (μm)	NS	1–10	20	7	5
Surface roughness (μm)	< 3.5	1.5–3.5	8	> 7.29	5
Laser specifications	Nd:YAG laser (CW) Power: 0.1–10 W Freq: 0.5–50 kHz	Nd:YAG laser (pulsed)	Fiber laser Power: 25 W/ 50 W	Pulsed laser Power: 30 W Freq: 1 kHz–1 MHz	NS
Spot size (μm)	25	25	19.4	30	30
Material	W, Al, Cu, Ag	W, Al, Cu, Ag, 316L, Mo, Ti, 80Ni20Cr	SS 316L	SS 316L	316L and 17-4PH
Powder particle size (μm)	0.3–10	1–10	5–25	3.5	D_{90}: 6
Environment	Vacuum (10^{-3} Pa) or reduced shield gas pressures (10^{4}–10^{5} Pa)	Vacuum (10^{-3} Pa)	O_2 < 300 ppm	Argon (O_2 & H_2O < 10 ppm)	Argon (O_2 & H_2O < 1 ppm)
Machine	Customized	Customized	NS	EOSINT μ60	DMP50GP

NS: not specified; Freq: frequency; D_{90}: the diameter of the particle that 90% of the particle distribution is below this value.

The Q-switched pulsed laser produced better resolution than the CW laser for ceramic materials, due to the non-accumulation of heat with the pulsed laser. Despite the successful sintering of certain metallic and ceramic materials using a laser micro sintering setup with Q-switched pulsed lasers, it can be perceived that pulsed lasers in micro SLM still possess limitations in terms of surface finish, melt pool stability, and defects. These limitations—along with the wide application of CW lasers in conventional SLM—could be the reason why most recent research works in this field have been carried out using CW lasers.

It should be noted that research efforts on micro SLM have been quite limited, and that this is disproportionate to the general enthusiasm that exists for the field of conventional macroscale SLM. For conventional SLM, the effects of various process parameters (as illustrated in Fig. 3) on the process characteristics have been widely reported in the literature [13,23,25,27,49,50]. Although micro SLM process parameters are expected to exhibit a significant influence on the process outcomes, including feature resolution, defects, surface finish, and microstructure, there are limited parametric studies on micro SLM available in the literature. Kniepkamp et al. [42] reported on the increase in the dimensional accuracy of certain part features with a reduction in laser power during the micro SLM of 316L powder. Fischer et al. [31] studied the formation of single tracks and bulk features using the micro SLM of 316L powder over a range of scanning speeds and laser powers, and the process window for homogeneous tracks and dense cuboids was identified. Abele and Kniepkamp [41] investigated the effects of the contour-scanning strategy, laser power, and scanning speed on the surface roughness and morphology of the vertical walls during the micro SLM of 316L powders. Contour scanning reduced the vertical surface roughness of the parts at the optimized exposure parameters. Despite these efforts, none of the previous research works on micro SLM/SLS have reported on the mechanical properties, microstructure, or residual stress profile of the fabricated features. Since the focus of those works was primarily on achieving fine dense features with a smooth surface, only characteristics such as feature resolution, part density, and surface finish were reported. Most of the components fabricated by means of conventional SLM have structural applications in which the mechanical properties and microstructural factors such as grain morphology and crystallographic texture are significant. Since the parts fabricated by means of micro SLM might also have requirements for the mechanical properties, residual stress, and microstructure, it is essential to understand the underlying behavior of the process.

Microstructure formation in SLM is influenced by a number of mechanisms including heat transfer, thermophysical properties of the materials, and phase transformations [51]. The mode of solidification and the resultant microstructure are controlled by the temperature gradient (G) and the liquid–solid interface velocity (i.e., solidification rate, R) of the melt pool, which are represented through solidification maps (G vs. R maps) [21]. The solidification modes are equiaxed dendritic, columnar dendritic, cellular, and planar. The commonly observed microstructure in SLM has been found to be columnar dendritic, as AM processes typically undergo rapid heating, solidification, and reheating during the melting of adjacent layers [7,11,21,51]. The predominant formation of columnar dendrites in SLM can be attributed to the large temperature gradient along the building direction [11]. The resulting microstructure in SLM is mainly controlled by process variables such as laser power, scanning speed, and scanning strategy, although a number of other factors including elemental composition, building direction, and part geometry also play a role [51]. Despite a vast quantity of literature being available on the resultant microstructure in conventional SLM, there have been no similar studies reported for micro SLM. In recent times, attempts have been made to investigate the effect of laser spot size (see Section 4.2) by defocusing the beam in PBF processes such as EBM and SLM. Al-Bermani [52] reported that defocusing the electron beam by changing the focus offset significantly influenced the melt pool morphology during the EBM of SS. A similar approach by Phan et al. [53] using a narrowly focused beam in the EBM of a cobalt (Co)-based alloy resulted in horizontal dendrites restricting the growth of typical columnar dendrites. McLouth et al. [54] studied the laser beam focus shift in the SLM of IN718, and observed that a smaller spot size produced finer and equiaxed microstructures due to higher power density. In our recent study on the single-track formation of 316L powder in micro SLM, the observed molten-pool morphology of a "double-crest" surface was quite different from that of the single tracks formed during macroscale SLM, due to the fine laser spot size in our research [55]. The above-mentioned research on defocusing effects indicates that the laser spot size may play a significant role in the process characteristics of micro SLM. Due to the finer spot size, smaller layer thickness, and finer powders in micro SLM, the microstructure formation is expected to differ from that of conventional SLM. Furthermore, as micro SLM involves a fine spot size, the temperature gradient and the solidification rate are expected to be higher, which may lead to faster cooling rates and hence to finer dendrites. Nevertheless, it is difficult to predict the microstructure of micro SLM, as it depends upon a number of factors involving complex mechanisms. The mechanical behavior of parts fabricated by means of conventional SLM, including the hardness, tensile, and fatigue properties of various materials, has been widely reported [11,25,50,56,57]. However, the mechanical properties of micro SLM parts have barely been investigated in the literature. The mechanical properties are typically influenced by defects, microstructure, residual stress, and post-heat treatment [7].

According to published reviews related to SLM or PBF in general, the following post-processing heat treatments are commonly used: stress relieving, aging, solution treating, and hot isostatic pressing (HIP) [7]. The motivation for heat treatment is to reduce or eliminate defects, control the microstructure, improve the properties, and relieve residual stresses [21,56,58]. HIP is typically used to close internal pores and cracks, whereas recrystallization refines the microstructure to equiaxed fine grains and aging controls precipitate formation [7,21]. Since SLM produces microstructures that are different from those formed by traditional processes, the heat treatment strategy is different as well [59–62]. As discussed earlier, micro SLM may result in microstructures that differ from those formed by conventional SLM due to the extremely fine spot size. Through suitable heat treatment, the microstructure is expected to be controlled while improving the mechanical properties. As the post-heat treatment for SLM components depends on a number of factors, including the initial microstructure, defects, residual stress, elemental composition, and desired output characteristics, it is challenging to predict a suitable heat treatment for micro SLM. Thus, future studies on the heat treatment of micro SLM will be very valuable, as they will bring significant opportunities to broaden relevant applications. First, however, it is necessary to understand the microstructure characteristics, such as grain morphology and phase formation, that are created by the micro SLM of various materials in order to identify optimized post-processing heat treatments.

Table 2 [63–68] compares various characteristics of commercially available AM systems for micromanufacturing in terms of the build volume, achievable layer thickness, laser specifications, laser spot size, recoating system, processing materials, and so on. The first commercial system for micro SLS was built over a patent [69] based on laser micro sintering [20,33]. The micro SLS process was commercialized as "EOSINT μ60" by 3D MicroPrint GmbH, a company founded by 3D-Micromac AG and EOS GmbH exclusively to develop micro SLS systems for metallic microfabrication. It can

Table 2
Benchmarking of commercially available AM systems for micromanufacturing.

	DMP64/EOSINT μ60 [63]	REALizer SLM 50/SLM 100 [64]	PRECIOUS M 080 [65]	MYSINT100 [66]	TruPrint 1000 [67]	ProX DMP 100 [68]
Manufacturer	3D MicroPrint GmbH	Realizer GmbH	EOS GmbH	Sisma SpA	TRUMPF	3D Systems, Inc.
Build volume (mm)	$L60 \times W60 \times H30$	$\phi70 \times H40$	$\phi80 \times H95$	$\phi100 \times H100$	$\phi100 \times H100$	$L100 \times W100 \times H100$
Layer thickness (μm)	1–5	20–50	30	20–40	10–50	NS
Laser specifications	Fiber laser; 50 W	Fiber laser; 20–120 W	Yb-fiber laser; 100 W	Fiber laser; 200 W	Fiber laser; 200 W	Fiber laser; 50 W
Laser spot size (μm)	< 30	~20	< 30	55/30	55	NS
Recoating system	Blade	Blade	Blade	Blade	Blade	Roller
Materials	SS, Ti, Mo, Al	CoCr, SS 316L, Ag, Au, Pd, Ti alloys	Ag, Au, Pd, Pt alloys	Precious metals, bronze, CoCr, SS, maraging steel, Ni alloys	SS, tool steel, CoCr, Al, Ni alloys, Ti, precious metals, bronze	CoCr, SS 17-4PH
Control environment	Argon	Argon	NS	Nitrogen, argon	Nitrogen, argon	Nitrogen, argon
Industry	Medical, jewelry, mechatronics, mold making, automotive	Jewelry, precision engineering	Watches, jewelry	Precious metal, jewelry	Medicine, dental, aerospace, energy, automotive	Precision engineering, research and development

be seen in Table 2 that the existing commercial systems have a laser spot size greater than or equal to 20 μm. It should be noted that this laser spot size must be reduced significantly in order to build precise parts. As the SLM/SLS process builds parts in a layer-by-layer fashion, it is necessary to achieve as small a layer thickness as possible in order to reduce the feature resolution. With the exception of EOSINT μ60, the other existing micro SLS systems typically produce a layer thickness between 10 and 50 μm, which cannot be used to achieve microfeatures with sub-micrometer dimensions. Despite different efforts to use various types of recoating systems, the commercial systems use either a blade or roller system, which is similar to macroscale SLM systems. The ability to reduce the layer thickness is correlated to the size of the powder used. Conventional SLM/SLS typically uses powders of 20–50 μm diameter, whereas micro SLS processes require particles with a diameter much smaller than 10 μm.

Recently, the authors (i.e., Singapore Institute of Manufacturing Technology, SIMTech) developed an in-house micro SLM system (Fig. 9(a)) with a fine laser spot size and a novel powder-recoating system with the ability to handle fine powders. Initial experimental results using SS 316L powders ($D_{50} \approx 10$ μm, in which D_{50} is the diameter of the particle that 50% of the particle distribution is below this value) demonstrate that the developed micro SLM system is capable of producing microfeatures with a fine surface finish. Various trials were conducted to validate the system by varying the laser power, scanning strategy, scanning speed, and hatching density. Fig. 9(b) shows various features that were fabricated using the micro SLM system with the following process parameters: a layer thickness of 10 μm, spot size of 15 μm, laser power of 50 W, scanning speed of 800–1400 mm·s^{-1}, and hatch spacing of 10 μm. At present, a minimum feature size of 60 μm and a minimum surface roughness (R_a) of 1.3 μm can be achieved. However, the system is capable of handling sub-micrometer and nanoscale powders to produce a layer thickness of 1 μm. With a further reduction in the layer thickness and powder particle size, a much finer feature resolution (< 15 μm) and a surface roughness of less than 1 μm could be achieved using the developed system.

Scaling down from conventional to micro SLM efforts necessitates certain considerations, which can be classified into ① equipment-related, ② process-related, and ③ post-treatment factors. Most of the process mechanisms and the effects of process parameters can be read across the scales. A fine spot size and particle size will naturally reduce the layer thickness and hatch

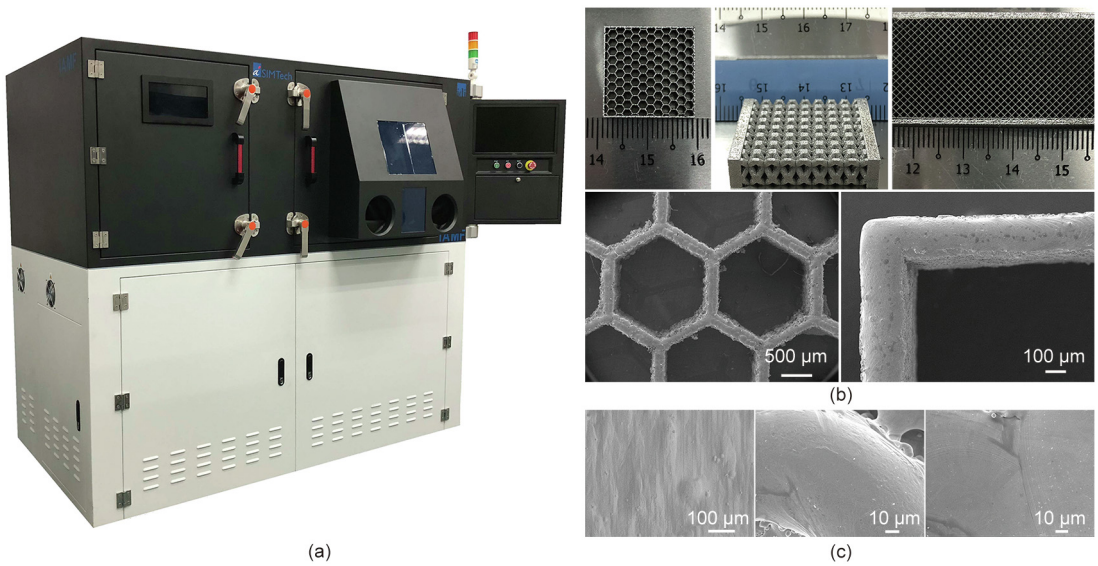

Fig. 9. (a) Micro SLM system developed by SIMTech; (b) various fabricated features using micro SLM; (c) scanning electron microscope (SEM) images of feature top surfaces.

spacing, leading to an increased process cycle time. Streek et al. [35] reported a 12-fold increase in the processing time of laser micro sintering to print the same component when the layer thickness and particle size were reduced by an order of magnitude. With the application of fine spots at microscales, the power density will be much higher. Therefore, the process throughput might be increased by using reduced laser power and/or faster scanning. Support structure design is another concern with micro SLM, as removing the structures is difficult and might affect the part dimensions. Similarly, preheating could be an issue in the case of high-aspect-ratio thin walls, especially when building support structures has been a difficulty.

Equipment-related scaling factors include the building platform, optical system, powder recoating, powder handling, and powder recycling. The size of the building platform and hence the entire equipment footprint is smaller for micro SLM systems. In order to satisfy one of the major requirements of achieving a fine spot size, the optical units must be modified, which will be described in Section 4.2. Another important requirement for micro SLM is achieving a smaller layer thickness, which can be realized by precision drives for the powder dispensing and building platform. The major equipment-related issues with the scaling down have been the need to use fine powders of the sub-micrometer scale or even nanoscale. Since the exposure of fine nanopowders to the environment carries safety and health hazards, it is advisable to minimize the manual handling of such powders. It is of the utmost necessity to provide a tight enclosure to the building chamber, as for any SLM machines. The effect of the powder particle size and the recoating system will be discussed in Sections 4.3 and 4.4, respectively. Post-treatment differences include the surface finishing and heat treatment performed on the AM parts. Heat treatment of microparts with thin features could result in part distortion. Powder adhesion to the walls has been a common occurrence in SLM, which necessitates further finishing after printing. In microscales, there is a possibility that the machining of thin walls will not be possible. A non-contact finishing such as electropolishing might be ineffective as well, as observed by Noelke et al. [38]. Thus, it is necessary to fabricate parts with a good surface finish both on the surface and along the walls, rather than relying on secondary subtractive processing. The surface-finishing effect is discussed in detail in Section 5.

4.2. Laser spot

Laser beam diameter is one of the most significant parameters influencing the feature resolution [31]. The minimum spot size, which occurs at the laser focal point, is typically used for AM processes, as the power density is maximized at the focus. PBF processes use a laser beam diameter in the range of 50–100 μm, whereas DED processes use millimeter-sized spots [21]. Ma et al. [70] studied the difference in the metallurgical behaviors of SS 316L fabricated by means of laser cladding deposition (LCD) and SLM, with the spot size of the LCD (> 1 mm) being much larger than that of the SLM (0.12–0.15 mm). SLM resulted in a higher depth-to-width ratio of the molten pool, higher cooling rate, smaller primary cellular arm spacing, lower grain aspect ratio, higher microhardness, and greater strength. Although it is difficult to attribute the SLM behavior to the beam diameter through this study, this work provides some indication of the consequences in terms of varying energy inputs, solidification rates, melt pools, and microstructure that result from a change in spot size. Liu et al. [71] investigated the effect of the laser beam diameter in SLM using SS 316L powders. For a reduction in beam diameter from 48 to 26 μm, improvements in the part density, surface finish, and mechanical properties were reported. Makoana et al. [72] used two different systems with different beam diameters (80 and 240 μm) to investigate the effect of spot size upscaling during laser-based PBF. The power density was kept constant in order to study the beam diameter effect. It was found that a smaller beam diameter and smaller laser power resulted in a narrower and shallower molten pool, leading to smaller hatch spacing and layer thickness.

Helmer et al. [73] studied the effect of spot size in EBM by changing the laser focus shift. The results indicated a significant difference in the melt pool geometry and microstructure for different spot sizes corresponding to the focused (400 μm) and defocused beam (500 μm). A recent paper by McLouth et al. [54] extended the analysis of a laser focus shift to SLM. IN718 samples fabricated at the focal point had a finer microstructure in comparison with the samples fabricated using the defocused beam. This behavior was attributed to a higher power density resulting from the smaller spot size. A concurrent study [74] on the effect of laser focus shift on porosity, surface roughness, and tensile strength reported a significant change in the built part properties with the focus shift. Varying melt behaviors ranging from a lack of fusion at the negative shift (−2 mm) to keyhole formation due to excessive energy at the positive shift (+3 mm) were observed. The change in energy input, along with the focus shift and spot size, corresponds to the divergence of the Gaussian distribution of the beam. However, it was noted that the optimum focus shift, and hence the spot size, is correlated to the scanning speed and laser power. Studies on a similar process—namely, laser welding—highlight the effect of smaller spots in improving welding behavior by achieving either a faster welding speed or deeper penetration, due to the increase in power density [75].

Despite extensive research efforts in SLM generally, it is noted that studies on the effect of spot size on the process behavior—especially on the feature resolution—is quite scarce. It can be seen in Table 1 that the spot size of micro SLM systems ranges from 20 to 30 μm, while the corresponding minimum feature resolution is similar to or slightly larger than the spot size. Similarly, commercial micro SLM systems have a laser spot size greater than 20 μm (Table 2). In order to realize fine microfeatures, it is necessary to achieve even finer beam spot sizes. DebRoy et al. [21] emphasized that small spot sizes and low power are required to achieve finer part resolution. The spot size is typically a function of the fiber core diameter, focusing lens, and collimator lens. Reducing the laser spot size is quite straightforward with an appropriate optical design. The optical system in SLM typically consists of a collimator, beam shaper, scanner, and objective F–θ lens. The scanning system in conventional and micro SLM machines typically uses a galvanometer, which consists of two mirrors, to guide the laser beam in at least two axes. In one of the first SLS systems, developed by Regenfuss et al. [32], a SCANLAB beam scanner with a scan field of 25 mm × 25 mm was used along with a Q-switched Nd:YAG laser with 0.1–10 W power in TEM_{00} mode. The optical design can also consist of other mechanisms, such as a digital mirror device, to achieve fine spot sizes [44]. However, a detailed review of optical systems is beyond the scope of this study.

4.3. Powders

Several powder characteristics (Fig. 3) influence the SLM process performance and, hence, the fabricated part quality. Powder shape, size, and surface roughness are the most significant parameters that influence the powder flowability and, consequently, the powder-bed properties, melt pool behavior, and part characteristics [76–78].

Olakanmi [79] studied the effect of powder properties on the SLM/SLS of pure Al and Al alloys. The results indicate that the shape of the powder particle has a significant effect on the processing maps and densification process. The powder particles with irregular shapes in the powders were found to exacerbate the formation

of agglomerates and porosity. An analysis of raw Ti–TiB powder shapes in SLM showed that irregularly shaped powder particles are detrimental to densification and, hence, to the tensile strength [80]. A study on powder characteristics by Cordova et al. [78] using different metal powders reported an occurrence of the maximum powder packing density with the most homogeneous morphology (i.e., most spherical). Liu et al. [71] observed that water-atomized 11 μm powder has a lower PBD compared with the apparent and tapped densities, due to the irregular angular morphology and the fine particle size. These studies demonstrate common agreement regarding the need to employ powder particles with a spherical shape for SLM and AM processes in general [7,76,77].

The influence of particle size in SLM has been widely investigated, as has been reviewed by Sutton et al. [76]. A smaller particle size typically results in better powder packing (increase in apparent density) and poor flowability [81]. In contrast, a poorer apparent density, tap density, and PBD were reported with finer IN718 powders [71]. Finer powders result in better surface roughness of the final part after SLM [82,83], but an increase in porosity [84]. Simchi [85] reported better part densification during SLM with a finer powder particle size or greater surface area, in the absence of agglomeration. An optimal powder particle size is dependent on other process variables, as the use of a powder particle size that is larger than the laser spot size and layer thickness typically results in non-uniform energy distributions, which further affect the melt pool behavior [86].

In addition to the particle size, the PSD significantly influences the SLM process [76,77]. Liu et al. [71] revealed that a wider PSD achieved better surface roughness and part density, whereas better hardness and tensile strength occurred with a narrower PSD. Identifying an optimum powder particle size and PSD is challenging, as fine powders with a narrow PSD result in agglomeration, whereas coarse powders with a wider PSD lead to segregation [85]. Furthermore, a number of studies [87–89] have emphasized that a bimodal or multimodal powder distribution increases the powder packing density and part density. Based on this advantage, Vaezi et al. [14] proposed a bimodal approach for the microscale binder jetting process to improve the part surface quality.

Conventional SLM/SLS typically uses powders with a particle diameter of 25–50 μm, whereas micro SLS processes require particles with a diameter much smaller than 10 μm. Microscale and sub-micrometer-scale powders have been tested in micro SLS systems, but exhibit limitations in terms of part quality [20,31]. Regenfuss et al. [33] used powders as fine as 0.3 μm for laser micro sintering process to produce the features shown in Fig. 7. Fischer et al. [31] used powders with a size of 3.5 μm, but the finest feature resolution was about 57 μm. To fabricate sub-micrometer features, nanopowders are necessary. However, nanopowders result in excessive agglomeration and oxidation due to the high surface-area-to-volume ratio [44]. Fig. 10 [33,90] shows the agglomeration of both irregularly shaped and fine spherical powder particles. Van der Waals forces become dominant over gravity at the nanoscale [90]. Agglomeration increases the interparticle friction and reduces the powder flowability, leading to inhomogeneous powder layering [76]. Further effects include the balling effect and an increase in porosity. In addition to agglomeration, fine powder particles result in a number of other issues that need to be resolved in the case of micro SLM system development:

- The reflectivity of fine powders is higher, which reduces the absorptivity of the laser irradiation during SLM.
- Nguyen et al. [82] observed that finer powders with a particle size less than a few micrometers were carried away by the inert gas flow during the SLM of IN718.
- Fine powders might vaporize at very high energy densities, leading to a reduction in part density, as was observed with SLM [71].
- Another drawback is the reactivity of the fine powder, which necessitates additional safety measures during handling and transportation.

4.4. Powder-recoating system

The major issue that has been reported for micro SLM/SLS for metals has been the inability of the traditional recoating systems to effectively deposit the powder on the powder bed. There is a common consensus on the need for innovative powder-recoating mechanisms that can homogenously spread powders at the sub-micrometer scale or nanoscale. However, as mentioned earlier, nanopowders are prone to excessive agglomeration due to the high surface-area-to-volume ratio and resulting high surface energy. At the nanoscale, van der Waals forces become dominant over gravity, leading to non-uniform powder layers during the recoating step of the AM process. In order to achieve efficient layering with a good powder packing density, one or more of the following approaches are needed for micro SLM:

- An effective powder distribution strategy to avoid powder clogging;
- Mechanical separation of agglomerated powders;
- Thermal energy to increase the packing density (preheating/pre-sintering);
- Use of an additional binding agent for effective distribution (slurry-based).

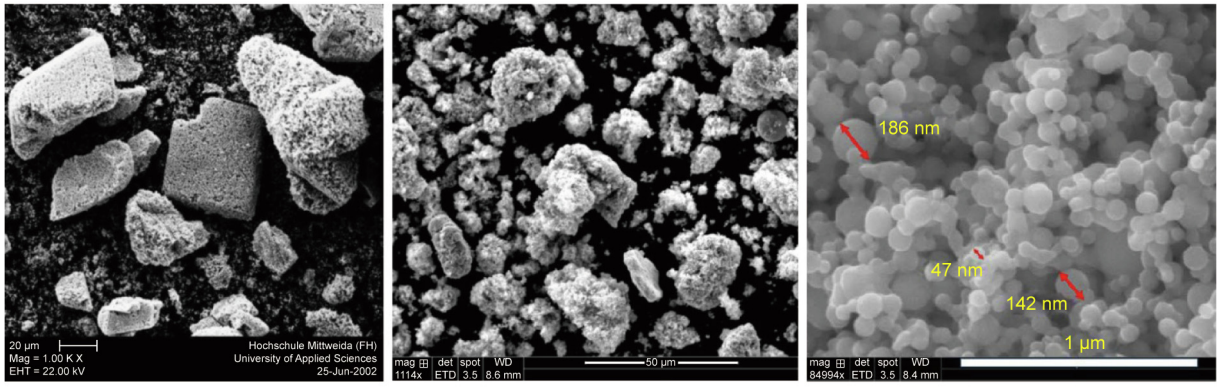

(a) (b) (c)

Fig. 10. Agglomeration of (a) sub-micrometer grained W powder; (b) Cu nanoparticles (average particle size of 100 nm) with an irregular shape; (c) spherical Cu nanoparticles with a size of 40 nm. (a) is reproduced from Ref. [33] with permission of Emerald Group Publishing Limited, © 2007; (b) and (c) are reproduced from Ref. [90] with permission of Elsevier B.V., © 2018.

In order to devise new powder distribution strategies that are not limited to micro SLM, it is necessary to understand the existing techniques that are currently used in conventional SLM.

4.4.1. Current raking methods

Powder-bed recoating depends on the flowability of the powder, which is influenced by a combination of the powder and equipment characteristics [91]. The flowability must be increased first for better powder distribution, whereas the powder needs to be intact after the spreading. Most commercial SLM/SLS systems use either a blade or roller for recoating the powder layers (Fig. 11) [20,45,92,93], as described in Table 2.

The most common spreading mechanism is raking with a doctor blade, as illustrated in Fig. 11(a). A doctor blade is simply a thin piece of metal or ceramic that is used to scrape the powder across the surface of a powder bed. Since the powder is not fluidized with the blade spreader, high shear forces are applied to the previously deposited layer [94]. Applying ultrasonic vibration to the blade is expected to reduce these shear stresses.

Rollers are the second most common device for powder raking. Translation of the roller across the powder bed, or clockwise rotation, produces a forward rotating motion, which is called a forward-rotating roller (FR), as shown in Fig. 11(b). This method tends to impart compaction of the powder, as there is more powder in front of the roller during its translation [91]. However, a lump of powder sticks to the roller during the forward motion and creates craters in the powder bed. Roller rotation in the opposite direction, called a counter-rotating roller (CR), has better flowability, as it forces the powder up while fluidizing the powder (Fig. 11(c)). However, there is no compaction of the powder with the CR method. Niino and Sato [92] proposed a combined setup of FR and CR, as shown in Fig. 11(d). The CR first scraps off the excess powder from the bed, which facilitates better compaction by the FR. Budding and Vaneker [91] replaced the CR with a doctor blade, in order to impart the same scraping effect while reducing the process time. However, their method still produced craters and drag on the powder bed. Roy and Cullinan [45] used a doctor blade and a CR instead, in order to provide raking and compaction, respectively. In the setup shown in Fig. 11(e), vibration of the CR was added to induce compaction of the powder that was first spread by the doctor blade. Haferkamp et al. [93] used a combination of three rollers to provide both the forward- and counter-rotating rolling action (Fig. 11(f)), where the layer thickness was controlled by the distance between the rollers. Regenfuss et al. [20] used a compaction cylinder in addition to the raking blades, in order to disperse and compact the fine powder used for micro-scale powder-bed processes. The schematic of the powder-raking system is illustrated in Fig. 11(g). In this setup, the build substrate, fused part, and remaining powder below the fresh powder layer are lifted upward toward a manual cap, in order to provide powder compaction. Table 3 [20,37,45,91–93] compares the different powder-raking systems described in the literature.

The existing raking systems are effective for the conventional SLM process, in which minor inaccuracies in the powder spreading can be considered negligible. At the microscale, however, similar issues could lead to a large deviation in the fabricated part dimensions. The effects would be exacerbated, as fine powders are used in micro SLM. Despite consistent efforts to improve the raking methods, they lack the required precision for micro SLM. The inability of existing recoating methods to achieve a homogeneous, dense layer of fine powder on the powder bed has consistently been reported [33,38,45]. The interaction between fine powder particles and the raking components greatly influence the efficiency of powder spreading.

The literature review reveals that raking systems are expected not only to disperse the powder onto the powder bed, but also to provide better volumetric packing density of the applied layer. Therefore, an effective powder-recoating system is required to control the layer thickness to sub-micrometer-scale or nanoscale precision while resulting in a homogeneous powder distribution along the powder bed.

4.4.2. Dry powder dispensing

In order to overcome the issues with the current powder distribution systems, Vaezi et al. [14] suggested dry powder-dispensing techniques, especially for microscale PBF processes. The mechanical methods of dry powder dispensing include the pneumatic, volumetric, and screw/auger methods, which have limitations such as a slow feed rate and an inability to handle fine powders [95]. The spatial resolution of these methods is at least two orders of magnitude lower than what is necessary for micro SLM.

Vibration methods have attracted increasing attention in the field of fine powder feeding. These methods use vibrational behavior to cause an increase in free volume, which improves the particle displacement [95]. The breaking of particle agglomerates can also be achieved through vibration. Matsusaka et al. [96] first used the vibration of a vertical capillary tube (as shown in Fig. 12(a)) to control the flow of fine alumina powder with a particle size of 20 μm and an irregular shape. Due to adhesiveness, the fine powder could not flow through the capillary tube entirely by gravity. When vibration was induced on the capillary tube through a variable direct current (DC) motor, it propagated into the powder, causing a reduction in frictional stress between the tube wall and the powder. Both the amplitude and the frequency of vibration are critical parameters affecting the flow rate. The powder flow rate is proportional to the frequency, but inversely proportional to the amplitude. The same research group used an ultrasonic transducer to induce vibration of the capillary tube [97]. A similar setup was developed by Yang and Evans [98] (as shown in Fig. 12(b)) to print polygonal-shaped tungsten carbide (WC) powder particles with a size of 12 μm on a substrate. Li et al. [99] used ultrasonic vibration generated by a piezoelectric transducer to feed 3 μm copper and SS powders. Because of the micro-vibrations in the ultrasonic frequency, the thin powder layer near the inner wall behaved as a lubricant. The benefits of ultrasonic powder feeding lie in its ability to prevent powder agglomeration and achieve continuous and uniform powder feeding, due to the traveling of the ultrasonic wave along the capillary tube. Yang and Evans [95] developed a system, as shown in Fig. 12(c), to mix and deposit multiple materials using individual powder hoppers and a mixing hopper, where the flow rate is controlled by acoustic vibration. These research works have demonstrated the capability of the ultrasonic-based micro-feeding devices which can be integrated with lasers and used in a typical AM system.

Another promising powder-feeding mechanism for AM is electrostatic-based dispensing. Electrostatic coating or spraying has been widely used for industrial coatings and in construction [100]. In recent times, it has found an application in the pharmaceutical dry coating of tablets, as detailed by Yang et al. [101] in a recent review. This method works on the principle of electrostatic attraction between opposite charges. As illustrated in Fig. 13(a) [101], the powder particles are charged while being exposed to a strong electrical field. The negatively charged particles are attracted to the substrate, which is either positively charged or grounded. In electrostatic spraying, the charging of powder occurs when powder particles pass through the spray gun, and are then deposited on the ground substrate. In comparison with other dry-coating methods, electrostatic coating greatly improves the coating efficiency and adhesion due to the electrical attraction.

Electrophotography is another common application using the electrostatic method, in which the photographic papers are printed with toner particles [102]. In electrophotography, a light-sensitive

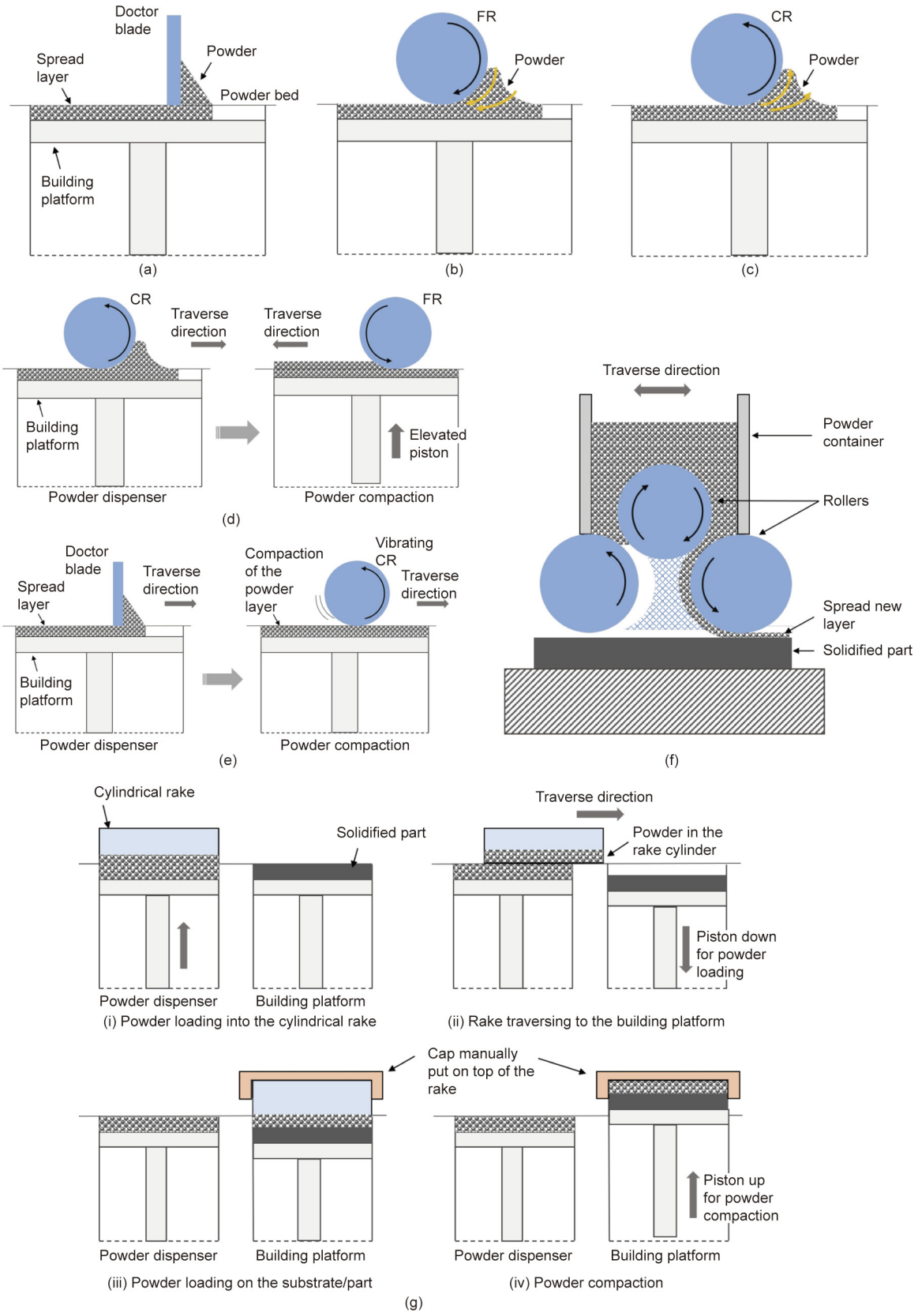

Fig. 11. Schematic of the existing raking systems in powder-bed AM. (a) Doctor blade; (b) forward-rotating roller (FR); (c) counter-rotating roller (CR); (d) combined FR–CR; (e) combined doctor blade and vibrating CR; (f) three-roller system; (g) cylindrical raking system with compaction. (d) is reproduced from Ref. [92] with permission of University of Texas at Austin, © 2009; (e) is reproduced from Ref. [45] with permission of University of Texas at Austin, © 2015; (f) is reproduced from Ref. [93] with permission of Elsevier B.V., © 2004; (g) is reproduced from Ref. [20] with permission of Wiley-VCH Verlag GmbH & Co. KGaA, © 2007.

Table 3
Comparison of powder-raking methods [20,37,45,91–93].

	Doctor blade (DB)	CR	FR	CR followed by FR [92]	DB followed by FR
Introduction	No real compaction occurs; only alters the layer height	Mostly for powder spreading, as less compaction occurs	More compaction, as more powder is under the roller	Limits the amount of powder in front of FR by initial compaction using CR	Replacement of CR by DB for a quicker operation
Advantages	Simple and easily controllable	Stimulates the powder flowability in front of the powder	Provides compaction	Both spreading and compaction	High throughput
Limitations	Unevenness of the blade affects the deposited layer; also, the powder is not fluidized	No significant compaction of the powder	A compressed lump of the powder sticks to the roller surface and causes craters	Long process cycle time	Distortions of the powder surface at a low density
Process parameters	Layer height, blade velocity	Linear and rotational speed of the roller, roller radius, angle, friction	Linear and rotational speed of the roller, roller radius, angle, friction	Linear and rotational speed of the rollers, roller size, friction	Blade and roller translation velocities, roller diameter

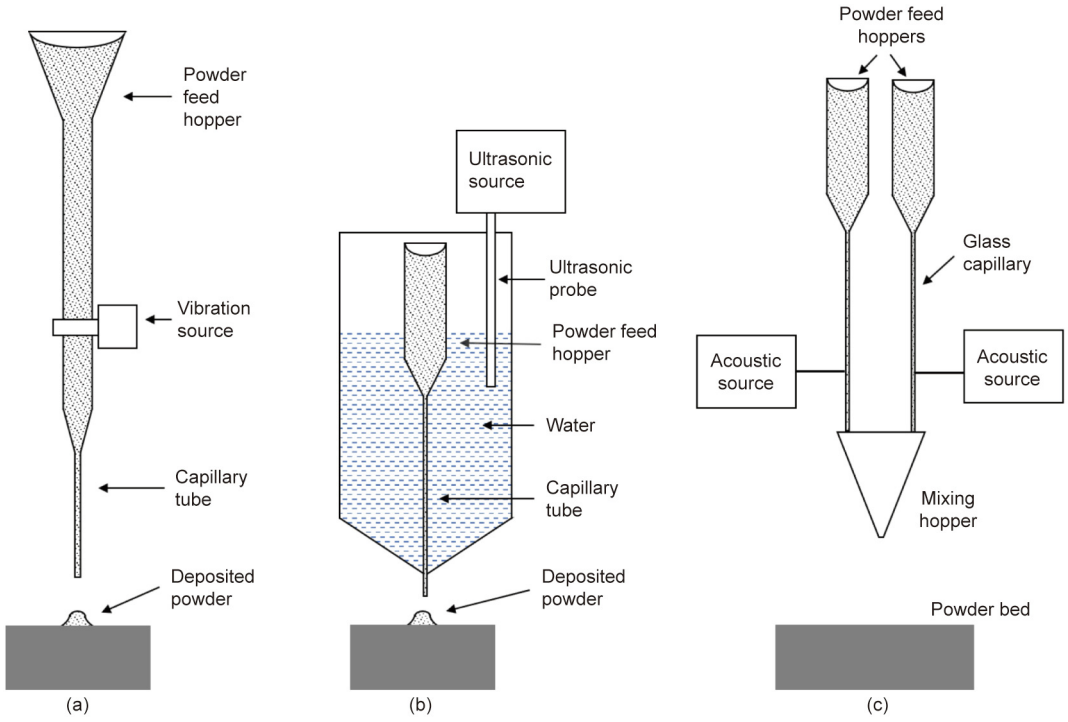

Fig. 12. Schematic of vibration dry powder-dispensing systems. (a) Vibration using a direct current motor; (b) vibration using an ultrasonic source; (c) multi-powder-dispensing system using acoustics for powder-bed AM. (a) is reproduced from Ref. [96] with permission of Society of Powder Technology Japan, © 1996; (b) is reproduced from Ref. [98] with permission of Elsevier B.V., © 2004; (c) is reproduced from Ref. [95] with permission of Society of Powder Technology Japan, © 2007.

photoconductor is first charged by a high voltage corona. The latent image is then created on the photoconductor by selectively discharging its surface through a light source. The charged toner particles are deposited on the photoconductor, which is then transferred to the paper. Based on the electrophotography technique, Liew et al. [103] developed a secondary powder-deposition system to be used for multi-material fabrication using SLS. In the simple experimental setup, a Teflon scraper was used to detach the negatively charged toner, which was then deposited over a paper with a positive charge. Kumar and Zhang [104] developed electrophotography-based powder deposition for powder-bed-based techniques such as SLM/SLS, which can also be applied for binder jetting [105]. A schematic of their setup is similar to that of the electrophotography process, which is shown in Fig. 13(b) [104]. Polystyrene powders with a particle size of 5 μm were deposited on an aluminum building platform and fused together by a heat roller to achieve parts with a thickness of 1 mm. In this technique, layer thickness was controlled by parameters such as the speed of the photoconductive belt, charge per unit mass of powder, and developing roller speed. Thomas et al. [106] also developed an electrophotography-based powder-deposition method for the SLM process. Their setup demonstrated a good transfer of polymer powders from the charging plate to the substrate. Both research works proposed multi-material powder deposition using electrophotography [104,106]. The deposition efficiency was found to be influenced by the electrical potential and by the distance between the charging plate and substrate. Despite the initial formation of a uniform monolayer of powders on the substrate, it was difficult to control the stacking of further layers, as is necessary for SLM, in electrophotography-based deposition. Two approaches are proposed in order to achieve powder deposition in a typical SLM process, which requires a constant potential between the photoconductor and the substrate or solidified part surface: ① removal of residual charge from the fused layers; and ② additional charging by a corona device in order to increase the charge density.

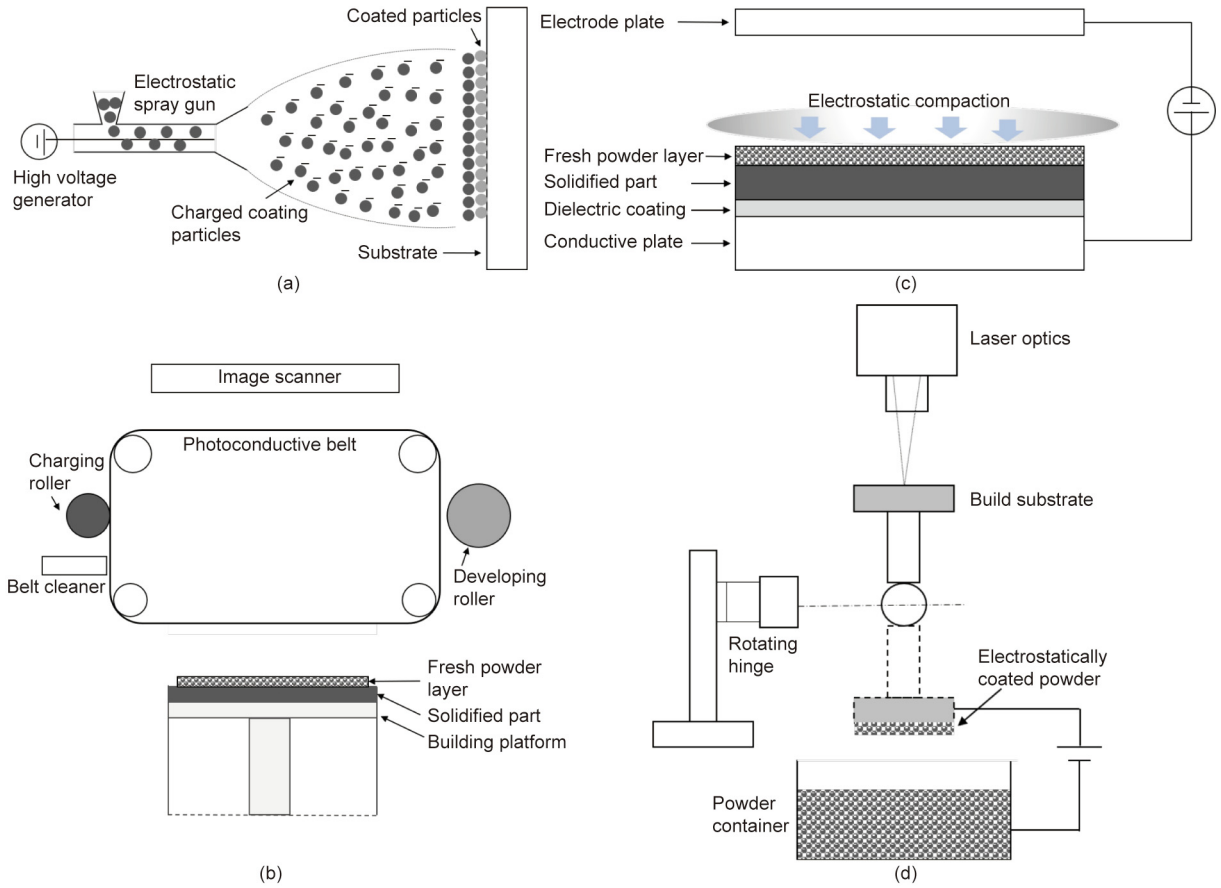

Fig. 13. Schematic of electrostatic dry powder-dispensing systems. (a) Electrostatic spraying; (b) electrophotography-based powder dispensing for SLM; (c) electrostatic powder compaction; (d) electrostatic powder dispensing for powder-bed AM. (a) is reproduced from Ref. [101] with permission of Chinese Society of Particuology and Institute of Process Engineering, CAS, © 2016; (b) is reproduced from Ref. [104] with permission of Laboratory for Freeform Fabrication and University of Texas at Austin, © 2018; (c) is reproduced from Ref. [109]; (d) is reproduced from Ref. [110].

A sieve feed system was designed by Melvin and Beaman [107] to be used in SLS. Unlike electrography, the sieve feed system works by the removal of static electric charges. In the sieve feed system, the powder is forced onto the powder bed through a charged or ground sieve, whereas leveling is performed by a squeegee or roller. An increase in the built part strength of 3 to 4 times and in the part density of 10%–15% was achieved after the sintering of polycarbonate powder using the sieve feed system, in comparison with roller feeding. The observed behavior was attributed to the corresponding increase in the PBD due to the removal of electrostatic charge from the powder passing through the sieve. However, this system has difficulty achieving precise layering and a uniform coating thickness. The same researchers developed an electrostatic-coating-based powder-recoating method for SLS [108]. Although the electrostatic powder layering produced better dispersion than the roller, the sintered part still had a significant amount of porosity.

A recent patent by Applied Materials Inc. [109] uses electrostatic charging to compact the spread powder layer with the base plate or the pre-sintered part, as illustrated in Fig. 13(c). Electrostatic compaction is applied when the potential drop at the gap between the electrode and the layer of fresh feed powder is larger than the potential drop across the layer of sintered and fresh feed material. Plasma, which is generated through the gas flow, can also be used to increase the compaction force. In this case, most of the potential drop occurs across any previously deposited layers and the layer of fresh feed material. Paasche et al. [110] conceptualized a powder-bed system for AM using electrostatic powder deposition, as illustrated in Fig. 13(d). In their setup, the positively charged substrate collects powder from the negatively charged powder container with the application of voltage. Once the powder is deposited, the substrate traverses toward the laser beam for subsequent melting. The process repeats until the entire part is fabricated. Once implemented, this system could have the following issues: ① Positioning the substrate at the focal spot for laser irradiation and at the specific location for powder deposition for every layer is time-consuming and could lead to errors; ② traversing the substrate between each layer might lead to positioning inaccuracies and part shifting; and ③ disposal of the trapped powders before the shifting may be difficult. In addition, the ability of this system to achieve further layering may still be lacking.

Despite the demonstrated feasibility of vibratory and electrostatic powder dispensing for precise and selective layering in powder-bed processes, these techniques have certain limitations:

(1) Powder dispensing through nozzle-based systems is strongly influenced by the process environment, and nozzle clogging will hamper reliable powder delivery.

(2) Dry powder-dispensing systems have a much higher deposition time than conventional powder-recoating methods. This will increase the process cycle time of the powder-bed processes, when AM is already tackling the issue of a much higher cycle time in comparison with conventional manufacturing processes.

4.5. Powder-bed characterization

For SLM at the microscale, the application of thin powder layers is a crucial step that can greatly affect the part resolution, surface finish, porosity, microstructure, and mechanical properties. Liu et al. [71] reported that the PBD significantly influences the

fabricated part density in SLS. It is notable that no process variable is available to compare the different powder-dispensing techniques. Any comparison—if it exists—is made through the sintered or melted part density. As SLM is comprised of a number of process parameters, it is difficult to segregate the effect of the powder-bed characteristics while comparing the final parts. This section provides details on PBD, as it is an influential factor in microscale powder-bed systems.

The packing of the powder during the powder-bed processing influences the part density. However, there is no standard procedure to characterize the density of the powder bed experimentally [111]. Elliott et al. [112] devised a method to characterize the density of the powder bed used for binder jet printing. First, a CR was used to deposit the powder on the powder bed. Next, a binder jet was applied along the contours of a cup, leaving loose powder in the cavity. After printing, the cups were removed and the weight of the loose powder was evaluated. The PBD could be calculated, as the weight and volume of the cup were known. A similar method was used by Liu et al. [71] for SLM, in which the PBD was measured by melting the walls of a square container. In both studies, the PBD was found to fall between the apparent density and tapped density of the powder. Gu et al. [81] devised a method to calculate the PBD without binders or sintering along a disc. An SS disk with a diameter of 60 mm was placed on the building platform of the sintering machine. Three layers of 0.03 mm thick powder were spread over it for each measurement, creating a total height of 0.09 mm. The volume of the powder, therefore, could be determined. The disk was then removed from the platter and weighed both with and without powder; the difference was the mass of the three layers of powder. The PBD was calculated using the mass and volume. No correlation between the powder flowability (angle of repose) and the PBD was observed from the results. In an experiment by Zocca et al. [113], the density of the powder bed was determined by weighing the powder after a deposition of 50 layers (each 100 μm thick) in the printer's building platform and dividing the mass by the geometrical volume obtained.

5. Surface finishing and hybrid processing

SLM-fabricated components generally have a surface roughness greater than 10 μm, which mandates post-processing [114]. Despite the drive to achieve smooth surfaces with a roughness of less than 1 μm, it might be inevitable that a secondary finishing is required for micro AM parts. This section first focuses on typical surface-finishing techniques that are used for AM components, and on the capabilities of such techniques. Next, it briefly discusses the suitability of these methods for application to micro SLM parts, whether as separate post-processing or through integration with the micro SLM to form a hybrid system.

Table 4 [115–127] compares some common surface-finishing techniques that are used for AM components. Traditional subtractive machining is typically used to improve the surface finish of the near-net shaped components produced by AM [7]. Simple mechanical grinding and/or polishing may be adequate for some applications, although they do not usually meet the standards required for high-quality parts [115].

Chemical and electrochemical polishing (ECP) have an advantage over conventional machining in terms of the ability to be used for complex features. Pyka et al. [118] used chemical etching (CHE) and ECP for titanium alloy-based open porous structures; it was found that CHE mainly removed the attached powder grains, while ECP reduced the roughness further. Alrbaey et al. [117] used ECP to reduce the roughness of SLM-made SS 316L from 10–17.5 to 0.5 μm. Yang et al. [128] electropolished Ti6Al4V samples fabricated by means of EBM, which resulted in a reduction of the surface roughness from 23 to 6 μm. Shape accuracy loss and inconsistent polishing across different regions and times were observed. ECP is limited by its tendency to erode the material, which results in dimensional inaccuracies, in addition to the associated environmental concerns [115].

Laser polishing or laser re-melting has emerged as a potential cost-effective surface-finishing process for SLM surfaces that can use the same laser source as AM [115,121,129]. Yasa et al. [129] achieved a final surface roughness of 1.5 μm after the laser re-melting of SLM-made SS 316L with an initial roughness of 12 μm. The laser polishing of additively manufactured SS AISI 420 infiltrated with bronze reduced the surface roughness (R_a) from 7.5–7.8 μm to values below 1.49 μm, with no cracks or pores in the heat-affected zone [120]. Ma et al. [121] observed a reduction in surface roughness from 5 μm to below 1 μm on Ti-based alloys. Marimuthu et al. [115] achieved a roughness reduction from 10.2 to 2.4 μm on SLM-manufactured Ti6Al4V, with no formation of the alpha case or thermal cracking. Despite the feasibility of laser polishing for AM components, this method is limited to flat surfaces and external features. In addition, surface re-melting can affect the surface chemistry and thermal residual stress.

Abrasive blasting—commonly known as sandblasting—is widely used in industry for cleaning surfaces, engraving, and deburring [130]. Sand, abrasives, and nut shells are used as the blasting media, which is propelled by pressurized air or fluid. De Wild

Table 4
Comparison of surface-finishing techniques for AM-fabricated parts.

Process	Capabilities (μm)	Advantages	Limitations	Eligibility for micro SLM	Ability for hybrid system
CNC machining	$R_a \approx 0.4$ [116]	Effective for simple geometries Can achieve a mirror finish	Difficult to machine complex structures Micro-tooling is time-consuming	Yes	Yes
CHE/ECP	$R_a \approx 0.5$ [117,118]	Easy to process internal channels and difficult-to-access areas	Dimensional inaccuracies due to material erosion Environmental concerns	Yes	No
Laser polishing	$R_a < 3$ [119] $R_a \approx 1.5$ [120] $R_a \approx 0.4$ [121] $R_a \approx 2.4$ [115]	Same laser source can be used Reduction in floor space	Difficult for internal features and inclined surfaces Re-melting could introduce thermal residual stresses and changes in surface chemistry	Yes	Yes
Abrasive blasting	$R_a < 1$ [122–124]	Simple, flexible technique	Poor process repeatability	Yes	No
Abrasive flow machining	$R_a < 1$ [125]	Can be used for internal and difficult-to-access features	Limited finish due to the abrasive flow direction	Yes	No
Mass finishing	$R_a < 1$ [126,127]	No tooling requirements Batch processing	No localized finishing High process cycle time	No	No

CNC: computer numerically controlled; CHE: chemical etching; ECP: electrochemical polishing.

et al. [122] used sandblasting to finish porous orthopedic Ti implants fabricated by means of SLM. The surface roughness (S_a) of the implant was reduced from 3.33 to 0.94 μm after sandblasting with corundum. Strickstrock et al. [131] used yttria tetragonal zirconia polycrystal (Y-TZP) particles to sandblast Y-TZP surfaces to produce a roughness of 1.7 μm. Klotz et al. [132] used sandblasting with corundum sand and glass beads to polish SLM-fabricated yellow-gold alloys from an initial roughness of 12.9 to 4.2 μm. Sandblasting was also used to improve the aesthetic appearance of SLM-made maraging steel [133]. Qu et al. [123] reported that the surface roughness of electrical discharge machining (EDM) rough-cut WC–Co parts were improved significantly by abrasive blasting, with the average surface roughness (R_a) falling from 1.3 to 0.7 μm. Table 5 [122–124,131,132,134] summarizes the effect of different abrasive blasting treatments on the final surface quality of various materials. It can be deduced that abrasive blasting can effectively reduce the surface roughness by 50%–70% with a minimum R_a of less than 1 μm. Despite the limitation of process repeatability, abrasive blasting is commonly used for microcomponents, as it is advantageous in terms of process simplicity, flexibility, cycle time, and cost.

A number of new and different techniques have been implemented for complex AM components in order to address the challenging surface-finishing requirements. Tan and Yeo [135] developed a new technique—ultrasonic cavitation abrasive finishing—for AM components. In this method, cavitation bubbles formed by ultrasonic pressure waves within a liquid medium were observed to remove the partially melted powders. The collapse of cavitation bubbles induces shock waves, which propagate the abrasive particles toward the sample surface, resulting in material removal. The surface roughness of as-received IN625 was reduced from 6.5–7.5 to 3.7 μm. Wang et al. [125] used abrasive flow machining (AFM), a well-known finishing technique that forces semisolid abrasive media across the surface, for SLM components. A significant improvement in the surface finish of SLM-made aluminum alloy was achieved after AFM, with a reduction in surface roughness from 14 to 0.94 μm. Magnetic abrasive finishing (MAF), which creates abrasion from magnetic forces acting on magnetic abrasives, was demonstrated to reduce the surface roughness of SS 316L internal channels from 0.6 to 0.01 μm [130]. A modified version of MAF—vibration-assisted magnetic abrasive polishing (VAMAP)—was explored by Guo et al. [136] to finish microchannels and grooves. A reduction in the surface finish from 2.2 to 0.3 μm was achieved along the micro-grooves using this process. Mass finishing techniques such as vibratory finishing [126,137] and barrel finishing [127], which are based on the principle of sliding between the component surface and the abrasive particles, have been used for AM parts. Vibratory finishing of SLM-fabricated Ti6Al4V with an average roughness of 17.9 μm led to a final roughness of 0.9 μm [126]. However, vibratory finishing resulted in a large number of roughness valleys on the surface. Boschetto et al. [127] used barrel finishing—a process in which material removal occurs through tumbling action due to a rotating barrel—to finish SLM-manufactured Ti6Al4V. A large reduction in surface roughness (from 13.3 to 0.2 μm with a 48 h process time) of SLM coupons was achieved using this technique. Despite its good surface-finishing performance and process simplicity, it is a time-consuming process.

In order to identify a suitable surface-finishing process for micro SLM components from the pool of available techniques discussed earlier, a number of factors must be considered, including initial roughness of the fabricated features, part size, geometry, minimum feature size resolution, process complexity, cycle time, and so forth. The size of micro SLM components is typically on the millimeter scale, whereas the minimum feature resolution is in the range of a few micrometers (Table 1). The eligibility of techniques to be used for micro SLM components is listed in Table 4. Despite achieving a good surface finish, mass finishing techniques might damage microscale features during the process. Computer numerically controlled (CNC) machining of micro SLM parts is feasible, but micro-tooling and tool path control for complex geometry present a difficulty. In particular, the micromachining of thin walls and of internal and high-aspect-ratio features is difficult and time-consuming. CHE and ECP typically require flat surfaces and cause material erosion along the edges, which might induce large dimensional inaccuracies in microparts. Abrasive blasting could be an ideal choice, as it is commonly used to finish the microparts that are fabricated in various industries such as dentistry and jewelry. Micro-abrasive blasting is one of the most frequently used surface treatments for a range of medical applications, such as obtaining the desired surface finish of dental implants to support osseointegration [122,131,138–140]. Kennedy et al. [124] used micro shot blasting with ceramic beads on high-speed steel (HSS) and coated carbides, which resulted in a 60% reduction of surface roughness, with the finest surface having an R_a of 0.4 μm. Laser polishing is another suitable candidate, although the thermal stresses caused by re-melting could result in part distortion, especially along thin features, due to residual stresses.

Hybrid manufacturing systems integrate AM with either subtractive or other assistive systems to improve the productivity and customization capability of the machine systems [141–143]. Hybrid systems in AM typically involve the integration of laser systems with CNC milling machines by mounting the laser cladding head (in case of LMD) to the *z*-axis of the milling machine [143]. Overall, the system design should improve the build capability, accuracy, and surface finish of the structures, with minimal post-processing. In the case of powder-bed fusion additive manufacturing (PBF-AM), hybrid systems are rarely available, with the exception of Sodick OPM250E and Matsuura LUMEX Avance-25 [144], although the surface quality of the components after PBF-AM has always been an issue [128]. Despite the many efforts that have been made toward microfabrication in powder-bed AM processing, no hybrid systems that include additive and subtractive machining have been developed to fabricate metallic materials at the microscale. In comparison with the finishing processes listed in Table 4, laser re-melting, or laser polishing, seems to be the most feasible

Table 5
Comparison of the effect of various abrasive blasting conditions on the surface finish.

Substrate material	Initial condition	Abrasive blasting media	Roughness, R_a or S_a (μm)		Reduction (%)	Ref.
			Initial	Final		
Ti implants	SLM	Corundum	3.3	0.9	72	[122]
Yellow-gold alloys	SLM	Corundum sand, glass beads	12.9	4.2	67	[132]
HSS, coated carbides	Milling/turning/drilling	Ceramic beads	1	0.4	60	[124]
WC–Co	EDM	SiC	1.3	0.7	46	[123]
TiN/Al_2O_3/TiCN coatings	CVD	Corundum	0.18	0.09	50	[134]
Y-TZP	Milling	Y-TZP particles	NS	1.7	NA	[131]

HSS: high-speed steel; CVD: chemical vapor deposition; NA: not available.

option for integration with micro SLM to develop a hybrid system. Either the same laser source or a different laser source can be used within the existing SLM system. Nevertheless, it should be acknowledged that every finishing technique has its own advantages and limitations, and selecting an ideal technique depends upon the initial conditions of the SLM-fabricated part and the finishing requirements. Therefore, it is rational to improve the capabilities of the SLM technique to fabricate features with a fine surface finish, in order to eliminate the need for any secondary finishing.

6. Potential applications

Micro AM—especially micro SLM—has found increasing application in the fabrication of precision devices and components in several fields. Microfluidic devices can be applied in the fields of cell biology, biomedical science, and clinical diagnostics [145]. The direct AM of microfluidic devices has been attempted, but the productivity of this method was found to be much lower than that of typical injection molding techniques [146,147]. The most common techniques for fabricating microfluidic devices are injection molding and hot embossing [148,149]. These techniques require a master mold or tool insert to replicate the features onto the substrate. Master molds for microfluidics are commonly fabricated using lithography, electroplating and moulding (LIGA, which is a German acronym for Lithographie, Galvanoformung, Abformung) and LIGA-like processes [150,151]. However, these techniques have material and design limitations. A metallic master mold can be fabricated using the electroforming of nickel, but the hardness of the mold is not sufficient [152,153]. The strength of the micro-molds manufactured by these techniques requires improvement. A precise micro AM technique for fabricating metallic micro-molds will improve the tool life and, hence, the productivity. The same technique can be used to produce high-aspect-ratio microstructures, which are increasingly finding application in MEMS [154]. Roy et al. [44] used a micro SLS process to fabricate electrical interconnect entities and dielectric build up in order to assemble integrated circuit (IC) packages. Silver electrodes and silver interconnects were printed on prefabricated traces to bridge two flexible substrates [16].

Another possible field for micro AM application is dentistry. At present, in addition to the most common stereolithography and digital light projection (DLP), SLM and SLS are used in dentistry [155,156]. Dental bridges and crowns, dental implants, partial dentures, and model castings are some of the potential applications of micro AM in the dental industry.

Over the past decade, there have been consistent attempts in the jewelry industry to manufacture jewelry using AM. This field is continuing to evolve, as almost all the major equipment makers for AM have stepped up their efforts to use AM to fabricate precious metals, such as gold, platinum, and palladium alloys [157]. In addition to common AM benefits such as near-net shape fabrication, decreased material wastage, and faster overall process cycle time for small batches, the specific attractive factors for jewelry are the ability of micro AM to fabricate thin-wall, filigree, meshed, and lightweight parts, thereby enhancing the design freedom and aesthetics. A number of studies from jewelry manufacturers [158,159] emphasized that despite the current limitations, SLM will coexist with traditional casting in order to realize design versatility and cost savings.

Hirt et al. [16] envisioned that devices and sensors could be directly printed onto existing technologies within the aeronautical, automotive, medical, and optical industries. The fabrication of components with microscale or nanoscale resolution helps to achieve a controlled microstructure. Precise microstructure control can be exploited to improve the mechanical strength and tribological properties of components fabricated using AM.

7. Concluding remarks

This paper systematically reviews the use of the SLM technique to achieve microscale features on metallic materials. Micro SLM is distinguished from conventional SLM by three factors: laser spot size, powder particle size, and layer thickness. The available research studies on micro SLM successfully demonstrate the feasibility of fabricating features with a microscale resolution on different materials including polymers, ceramics, and metals. Current micro SLM systems achieve a minimum feature resolution of 15 μm, minimum surface roughness of 1 μm, and maximum part density of 99.3%. Given the limited academic research in this field, it is surprising that there are a few commercial micro SLM systems on the market already. Commercial systems achieve a minimum spot size and layer thickness of 20 and 1 μm, respectively. One major limitation of the existing literature is that none of the works have attempted to investigate the physical properties and microstructure of the fabricated parts, which makes it difficult to compare the SLM process across scales.

In order to develop micro SLM technology, certain modifications to SLM systems are necessary, such as adjusting the optical system, powder recoating, and the drives for the powder dispensing and build stage. The current limitations to obtaining a thin and homogeneous powder layer are mainly the powder properties and powder-recoating system. The literature implies that the current powder-recoating methodology, which is predominantly performed by means of a blade or roller, is unsuitable for handling fine powders. This paper reviews a number of potential dry powder dispensing methods for their feasibility in powder-bed AM systems. Of the vibratory and electrostatic-based powder-dispensing methods that have already been implemented and tested in AM systems, electrostatic techniques seem to be most promising in terms of the coating cycle time. An effective strategy for micro SLM would be to integrate all the subsystems—such as powder dispensing, collection, and powder sieving—and have a closed-loop feedback system.

The surface-finishing techniques used for SLM parts have been reviewed in detail. Although most of the processes can achieve a surface roughness of less than 1 μm, the selection of an ideal process for micro SLM is based on a number of factors, including part geometry, feature resolution, and finishing requirement. The literature reveals that abrasive blasting is currently a common finishing technique for miniature parts. In an approach toward hybrid processing, the use of laser polishing as the secondary finishing technique for micro SLM appears to be more practical than other techniques.

Not limited to SLM/SLS, the common factors that restrict the application of micro AM are finite powder particle size, low confinement of the heating zone due to high heat dissipation in metals, difficulty in controlling the resolution, surface roughness, powder handling, and part removal [14,16]. These factors highlight the need to develop new systems with an innovative approach in powder distribution and post-processing of the built parts.

The future direction of micro SLM should be focused on two aspects: equipment-related and process-related factors. A system should be designed to handle nanoscale metal powders, which tend to agglomerate easily. The major focus should be on developing an innovative powder-recoating system that can achieve homogenous powder layers with sub-micrometer scale thickness, while simultaneously not compromising on the recoating speed. Regarding process knowledge, more studies are required in order to understand the interaction between nanoscale powder particles and the laser beam. Further understanding of the microstructure and mechanical properties of parts fabricated using micro SLM are needed due to the current limited number of studies. Considering the growing application for metallic microparts with fine features in various fields, including precision engineering, biomedical science, dentistry, and jewelry, further improvement in micro SLM will expand the scope of SLM or even of AM in general.

Acknowledgements

The authors would like to acknowledge financial support from the Science and Engineering Research Council, Agency for Science, Technology and Research (A*STAR), Singapore (142 68 00088).

Compliance with ethics guidelines

Balasubramanian Nagarajan, Zhiheng Hu, Xu Song, Wei Zhai, and Jun Wei declare that they have no conflict of interest or financial conflicts to disclose.

References

[1] Qin Y, Brockett A, Ma Y, Razali A, Zhao J, Harrison C, et al. Micro-manufacturing: research, technology outcomes and development issues. Int J Adv Manuf Technol 2010;47(9–12):821–37.
[2] Alting L, Kimura F, Hansen HN, Bissacco G. Micro engineering. CIRP Ann 2003;52(2):635–57.
[3] Jain VK, Sidpara A, Balasubramaniam R, Lodha GS, Dhamgaye VP, Shukla R. Micromanufacturing: a review—part I. Proc Inst Mech Eng Part B 2014;228(9):973–94.
[4] Gao W, Zhang Y, Ramanujan D, Ramani K, Chen Y, Williams CB, et al. The status, challenges, and future of additive manufacturing in engineering. Comput-Aided Des 2015;69:65–89.
[5] Huang Y, Leu MC, Mazumder J, Donmez A. Additive manufacturing: current state, future potential, gaps and needs, and recommendations. J Manuf Sci Eng 2015;137(1):014001.
[6] Gu DD, Meiners W, Wissenbach K, Poprawe R. Laser additive manufacturing of metallic components: materials, processes and mechanisms. Int Mater Rev 2012;57(3):133–64.
[7] Sames WJ, List FA, Pannala S, Dehoff RR, Babu SS. The metallurgy and processing science of metal additive manufacturing. Int Mater Rev 2016;61(5):315–60.
[8] Obikawa T, Yoshino M, Shinozuka J. Sheet steel lamination for rapid manufacturing. J Mater Process Technol 1999;89–90:171–6.
[9] Herzog D, Seyda V, Wycisk E, Emmelmann C. Additive manufacturing of metals. Acta Mater 2016;117:371–92.
[10] Gibson I, Rosen D, Stucker B. Binder jetting. In: Additive manufacturing technologies: 3D printing, rapid prototyping, and direct digital manufacturing. New York: Springer; 2015. p. 205–18.
[11] Fayazfar H, Salarian M, Rogalsky A, Sarker D, Russo P, Paserin V, et al. A critical review of powder-based additive manufacturing of ferrous alloys: process parameters, microstructure and mechanical properties. Mater Des 2018;144:98–128.
[12] Vilar R. Laser cladding. J Laser Appl 1999;11(2):64–79.
[13] Kruth JP, Badrossamay M, Yasa E, Deckers J, Thijs L, Van Humbeeck J. Part and material properties in selective laser melting of metals. In: Proceedings of the 16th International Symposium on Electromachining; 2010 Apr 19–23; Shanghai, China; 2010. p. 3–14.
[14] Vaezi M, Seitz H, Yang S. A review on 3D micro-additive manufacturing technologies. Int J Adv Manuf Technol 2013;67(5–8):1721–54.
[15] Engstrom DS, Porter B, Pacios M, Bhaskaran H. Additive nanomanufacturing—a review. J Mater Res 2014;29(17):1792–816.
[16] Hirt L, Reiser A, Spolenak R, Zambelli T. Additive manufacturing of metal structures at the micrometer scale. Adv Mater 2017;29(17):1604211.
[17] Bertsch A, Renaud P. Microstereolithography. In: Bártolo P, editor. Stereolithography. Boston: Springer; 2011. p. 81–112.
[18] Ko SH, Chung J, Hotz N, Nam KH, Grigoropoulos CP. Metal nanoparticle direct inkjet printing for low-temperature 3D micro metal structure fabrication. J Micromech Microeng 2010;20(12):125010.
[19] Gokuldoss PK, Kolla S, Eckert J. Additive manufacturing processes: selective laser melting, electron beam melting and binder jetting-selection guidelines. Materials (Basel) 2017;10(6):672.
[20] Regenfuss P, Ebert R, Exner H. Laser micro sintering—a versatile instrument for the generation of microparts. Laser Tech J 2007;4(1):26–31.
[21] DebRoy T, Wei HL, Zuback JS, Mukherjee T, Elmer JW, Milewski JO, et al. Additive manufacturing of metallic components—process, structure and properties. Prog Mater Sci 2018;92:112–224.
[22] AlMangour B, Grzesiak D, Yang JM. Selective laser melting of TiB_2/316L stainless steel composites: the roles of powder preparation and hot isostatic pressing post-treatment. Powder Technol 2017;309:37–48.
[23] Yakout M, Elbestawi MA, Veldhuis SC. On the characterization of stainless steel 316L parts produced by selective laser melting. Int J Adv Manuf Technol 2018;95(5–8):1953–74.
[24] Yasa E, Kruth JP. Microstructural investigation of selective laser melting 316L stainless steel parts exposed to laser re-melting. Procedia Eng 2011;19:389–95.
[25] Tucho WM, Lysne VH, Austbø H, Sjolyst-Kverneland A, Hansen V. Investigation of effects of process parameters on microstructure and hardness of SLM manufactured SS316L. J Alloys Compd 2018;740:910–25.
[26] Nguyen QB, Luu DN, Nai SML, Zhu Z, Chen Z, Wei J. The role of powder layer thickness on the quality of SLM printed parts. Arch Civ Mech Eng 2018;18(3):948–55.
[27] Cherry JA, Davies HM, Mehmood S, Lavery NP, Brown SGR, Sienz J. Investigation into the effect of process parameters on microstructural and physical properties of 316L stainless steel parts by selective laser melting. Int J Adv Manuf Technol 2015;76(5–8):869–79.
[28] Li R, Liu J, Shi Y, Du M, Xie Z. 316L stainless steel with gradient porosity fabricated by selective laser melting. J Mater Eng Perform 2010;19(5):666–71.
[29] Zhong Y, Liu L, Wikman S, Cui D, Shen Z. Intragranular cellular segregation network structure strengthening 316L stainless steel prepared by selective laser melting. J Nucl Mater 2016;470:170–8.
[30] Emmelmann C, Kranz J, Herzog D, Wycisk E. Laser additive manufacturing of metals. In: Schmidt V, Belegratis MR, editors. Laser technology in biomimetics: basics and applications. Berlin: Springer; 2013. p. 143–62.
[31] Fischer J, Kniepkamp M, Abele E. Micro laser melting: analyses of current potentials and restrictions for the additive manufacturing of micro structures. In: Proceedings of the 25th Annual International Solid Freeform Fabrication (SFF) Symposium; 2014 Aug 4–6; Austin, TX, USA; 2014, p. 22–35.
[32] Regenfuss P, Hartwig L, Klötzer S, Ebert R, Exner H. Microparts by a novel modification of selective laser sintering. In: Proceedings of Rapid Prototyping and Manufacturing Conference; 2003 May 12–15; Chicago, IL, USA; 2003. p. 1–7.
[33] Regenfuss P, Streek A, Hartwig L, Klötzer S, Brabant T, Horn M, et al. Principles of laser micro sintering. Rapid Prototyping J 2007;13(4):204–12.
[34] Regenfuss P, Hartwig L, Klötzer S, Ebert R, Brabant T, Petsch T, et al. Industrial freeform generation of microtools by laser micro sintering. Rapid Prototyping J 2005;11(1):18–25.
[35] Streek A, Regenfuss P, Ebert R, Exner H; Fachbereich MPI Laserapplikationszentrum. Laser micro sintering—a quality leap through improvement of powder packing. In: Proceedings of the 19th Annual International Solid Freeform Fabrication Symposium; 2008 Aug 13–15; Austin, TX, USA; 2008. p. 297–308.
[36] Exner H, Horn M, Streek A, Ullmann F, Hartwig L, Regenfuß P, et al. Laser micro sintering: a new method to generate metal and ceramic parts of high resolution with sub-micrometer powder. Virtual Phys Prototyp 2008;3(1):3–11.
[37] Gieseke M, Senz V, Vehse M, Fiedler S, Irsig R, Hustedt M, et al. Additive manufacturing of drug delivery systems. Biomed Tech 2012;57(Suppl 1):398–401.
[38] Noelke C, Gieseke M, Kaierle S. Additive manufacturing in micro scale. J Laser Appl 2013;2013(1):1–6.
[39] Dudziak S, Gieseke M, Haferkamp H, Barcikowski S, Kracht D. Functionality of laser-sintered shape memory micro-actuators. Phys Procedia 2010;5:607–15.
[40] Yadroitsev I, Bertrand P. Selective laser melting in micro manufacturing. In: Katalinic B, editor. Annals of DAAAM for 2010 & Proceedings of the 21st International DAAAM Symposium. Vienna: DAAAM International; 2010.
[41] Abele E, Kniepkamp M. Analysis and optimisation of vertical surface roughness in micro selective laser melting. Surf Topogr Metrol Prop 2015;3:034007.
[42] Kniepkamp M, Fischer J, Abele E. Dimensional accuracy of small parts manufactured by micro selective laser melting. In: Bourell DL, editor. Proceedings of the 27th Annual International Solid Freeform Fabrication Symposium; 2016 Aug 8–10; Austin, TX, USA; 2016. p. 1530–7.
[43] Roberts RC, Tien NC. 3D printed stainless steel microelectrode arrays. In: Proceedings of 2017 19th International Conference on Solid-State Sensors, Actuators and Microsystems; 2017 June 18–22; Kaohsiung, China. New York: IEEE; 2017. p. 1233–6.
[44] Roy N, Foong C, Cullinan M. Design of a micro-scale selective laser sintering system. In: Proceedings of the 27th Annual International Solid Freeform Fabrication Symposium; 2016 Aug 8–10; Austin, TX, USA; 2016. p. 1495–508.
[45] Roy N, Cullinan M. μ-SLS of metals: design of the powder spreader, powder bed actuators and optics for the system. In: Proceedings of the 26th Annual International Solid Freeform Fabrication Symposium; 2015 Aug 10–12; Austin, TX, USA; 2015. p. 134–55.
[46] Roy N, Dibua OG, Cullinan M. Effect of bed temperature on the laser energy required to sinter copper nanoparticles. JOM 2018;70(3):401–6.
[47] Ke L, Zhu H, Yin J, Wang X. Effects of peak laser power on laser micro sintering of nickel powder by pulsed Nd:YAG laser. Rapid Prototyping J 2014;20(4):328–35.
[48] Regenfuss P, Streek A, Ullmann F, Kühn C, Hartwig L, Horn M, et al. Laser micro sintering of ceramic materials: part 2. Interceram 2008;57(1):6–9.
[49] Yadroitsev I, Bertrand P, Smurov I. Parametric analysis of the selective laser melting process. Appl Surf Sci 2007;253(19):8064–9.
[50] Liverani E, Toschi S, Ceschini L, Fortunato A. Effect of selective laser melting (SLM) process parameters on microstructure and mechanical properties of 316L austenitic stainless steel. J Mater Process Technol 2017;249:255–63.
[51] Collins PC, Brice DA, Samimi P, Ghamarian I, Fraser HL. Microstructural control of additively manufactured metallic materials. Annu Rev Mater Res 2016;46(1):63–91.
[52] Al-Bermani SS. An investigation into microstructure and microstructural control of additive layer manufactured Ti-6Al-4V by electron beam melting [dissertation]. Sheffield: University of Sheffield; 2011.
[53] Phan MAL, Fraser D, Gulizia S, Chen ZW. Horizontal growth direction of dendritic solidification during selective electron beam melting of a Co-based alloy. Mater Lett 2018;228:242–5.

[54] McLouth TD, Bean GE, Witkin DB, Sitzman SD, Adams PM, Patel DN, et al. The effect of laser focus shift on microstructural variation of Inconel 718 produced by selective laser melting. Mater Des 2018;149:205–13.
[55] Hu Z, Nagarajan B, Song X, Huang R, Zhai W, Wei J. Formation of SS316L single tracks in micro selective laser melting: surface, geometry, and defects. Adv Mater Sci Eng 2019;2019:1–9.
[56] Lewandowski JJ, Seifi M. Metal additive manufacturing: a review of mechanical properties. Annu Rev Mater Res 2016;46:151–86.
[57] Suryawanshi J, Prashanth KG, Ramamurty U. Mechanical behavior of selective laser melted 316L stainless steel. Mater Sci Eng A 2017;696:113–21.
[58] Mohd Yusuf SYB, Gao N. Influence of energy density on metallurgy and properties in metal additive manufacturing. Mater Sci Technol 2017;33 (11):1269–89.
[59] Song B, Zhao X, Li S, Han C, Wei Q, Wen S, et al. Differences in microstructure and properties between selective laser melting and traditional manufacturing for fabrication of metal parts: a review. Front Mech Eng 2015;10(2):111–25.
[60] Gharbi O, Jiang D, Feenstra DR, Kairy SK, Wu Y, Hutchinson CR, et al. On the corrosion of additively manufactured aluminium alloy AA2024 prepared by selective laser melting. Corros Sci 2018;143:93–106.
[61] Amato KN, Gaytan SM, Murr LE, Martinez E, Shindo PW, Hernandez J, et al. Microstructures and mechanical behavior of Inconel 718 fabricated by selective laser melting. Acta Mater 2012;60(5):2229–39.
[62] Zhang H, Zhu H, Nie X, Qi T, Hu Z, Zeng X. Fabrication and heat treatment of high strength Al-Cu-Mg alloy processed using selective laser melting. In: Gu B, Helvajian H, Piqué A, editors. Proceedings of the SPIE 9738, Laser 3D Manufacturing III; 2016 Feb 13–18; San Francisco, CA, USA; 2016.
[63] DMP60 series [Internet]. Chemnitz: 3D MicroPrint GmbH; c2019 [cited 2018 Jun 30]. Available from: http://www.3dmicroprint.com/products/machines/dmp60-series/.
[64] Gebhardt A, Schmidt FM, Hötter JS, Sokalla W, Sokalla P. Additive manufacturing by selective laser melting the realizer desktop machine and its application for the dental industry. Physics Procedia 2010;5:543–9.
[65] Precious M 080 [Internet]. Krailling: EOS GmbH Electro Optical Systems; [cited 2018 Jun 30]. Available from: https://www.eos.info/precious-m-080.
[66] Mysint100, 3D selective laser fusion printer for metal powder [Internet]. Vicenza: Sisma SpA; [cited 2018 Jun 30]. Available from: http://www.sisma.com/eng/industry/prodotti/additive-manufacturing/laser-metal-fusion/mysint100.php.
[67] TruPrint 1000 [Internet]. Taicang: TRUMPF; c2019 [cited 2018 Jun 30]. Available from: http://www.trumpf-laser.com/en/products/3d-printing-systems/truprint-series-1000.html.
[68] Direct Metal Printers [Internet]. 3D Systems, Inc; c2017 [cited 2018 Jun 30]. Available from: https://www.3dsystems.com/sites/default/files/2017-01/3D-Systems_DMP_Tech_Specs_USEN_2017.01.23_WEB.pdf.
[69] Ebert R, Exner H, Hartwig L, Keiper B, Klötzer S, Regenfuss P, inventors; 3D-MICROMAC AG, assignee. Method and device for producing miniature objects or microstructured objects. United States patent US20070145629A1. 2007 Jun 28.
[70] Ma M, Wang Z, Zeng X. A comparison on metallurgical behaviors of 316L stainless steel by selective laser melting and laser cladding deposition. Mater Sci Eng A 2017;685:265–73.
[71] Liu B, Wildman R, Tuck C, Ashcroft I, Hague R. Investigation the effect of particle size distribution on processing parameters optimisation in selective laser melting process. In: Proceedings of the 22nd Annual International Solid Freeform Fabrication Symposium; 2011 Aug 8–10; Austin, TX, USA; 2011. p. 227–38.
[72] Makoana N, Yadroitsava I, Möller H, Yadroitsev I. Characterization of 17–4PH single tracks produced at different parametric conditions towards increased productivity of LPBF systems—the effect of laser power and spot size upscaling. Metals 2018;8(7):475.
[73] Helmer HE, Körner C, Singer RF. Additive manufacturing of nickel-based superalloy Inconel 718 by selective electron beam melting: processing window and microstructure. J Mater Res 2014;29(17):1987–96.
[74] Bean GE, Witkin DB, McLouth TD, Patel DN, Zaldivar RJ. Effect of laser focus shift on surface quality and density of Inconel 718 parts produced via selective laser melting. Addit Manuf 2018;22:207–15.
[75] Verhaeghe G, Hilton P. The effect of spot size and laser beam quality on welding performance when using high-power continuous wave solid-state lasers. In: Proceedings of the 24th International Congress on Applications of Lasers & Electro-Optics; 2005 Oct 31–Nov 3; Miami, FL, USA; 2005. p. 264–71.
[76] Sutton AT, Kriewall CS, Leu MC, Newkirk JW. Powders for additive manufacturing processes: characterization techniques and effects on part properties. In: Proceedings of the 27th Annual International Solid Freeform Fabrication Symposium; 2016 Aug 8–10; Austin, TX, USA; 2016. p. 1004–30.
[77] Spierings AB, Voegtlin M, Bauer T, Wegener K. Powder flowability characterisation methodology for powder-bed-based metal additive manufacturing. Prog Addit Manuf 2016;1(1–2):9–20.
[78] Cordova L, Campos M, Tinga T. Powder characterization and optimization for additive manufacturing. In: Proceedings of the VI Congreso Nacional de Pulvimetalurgia y I Congreso Iberoamericano de Pulvimetalurgia; 2017 Jun 7–9; Ciudad Real, Spain; 2017.
[79] Olakanmi EO. Selective laser sintering/melting (SLS/SLM) of pure Al, Al–Mg, and Al–Si powders: effect of processing conditions and powder properties. J Mater Process Technol 2013;213(8):1387–405.
[80] Attar H, Prashanth KG, Zhang LC, Calin M, Okulov IV, Scudino S, et al. Effect of powder particle shape on the properties of *in situ* Ti–TiB composite materials produced by selective laser melting. J Mater Sci Technol 2015;31(10):1001–5.
[81] Gu H, Gong H, Dilip JJS, Pal D, Hicks A, Doak H, et al. Effects of powder variation on the microstructure and tensile strength of Ti6Al4V parts fabricated by selective laser melting. In: Proceedings of the 25th Annual International Solid Freeform Fabrication Symposium; 2014 Aug 4–6; Austin, TX, USA; 2014. p. 4–6.
[82] Nguyen QB, Nai MLS, Zhu Z, Sun CN, Wei J, Zhou W. Characteristics of Inconel powders for powder-bed additive manufacturing. Engineering 2017;3 (5):695–700.
[83] Spierings AB, Herres N, Levy G. Influence of the particle size distribution on surface quality and mechanical properties in additive manufactured stainless steel parts. In: Proceedings of the 21st Annual International Solid Freeform Fabrication Symposium; 2010 Aug 9–11; Austin, TX, USA; 2010. p. 195–202.
[84] Parteli EJR, Pöschel T. Particle-based simulation of powder application in additive manufacturing. Powder Technol 2016;288:96–102.
[85] Simchi A. The role of particle size on the laser sintering of iron powder. Metall Mater Trans B 2004;35(5):937–48.
[86] Meier C, Penny RW, Zou Y, Gibbs JS, Hart AJ. Thermophysical phenomena in metal additive manufacturing by selective laser melting: fundamentals, modeling, simulation and experimentation. 2017. arXiv:1709.09510.
[87] German RM. Prediction of sintered density for bimodal powder mixtures. Metall Trans A 1992;23(5):1455–65.
[88] Karapatis NP, Egger G, Gygax PE, Glardon R. Optimization of powder layer density in selective laser sintering. In: Proceedings of the 10th Annual International Solid Freeform Fabrication Symposium; 1999 Aug 9–11; Austin, TX, USA; 1999. p. 255–64.
[89] Tan JH, Wong WLE, Dalgarno KW. An overview of powder granulometry on feedstock and part performance in the selective laser melting process. Addit Manuf 2017;18:228–55.
[90] Roy NK, Foong CS, Cullinan MA. Effect of size, morphology, and synthesis method on the thermal and sintering properties of copper nanoparticles for use in microscale additive manufacturing processes. Addit Manuf 2018;21:17–29.
[91] Budding A, Vaneker THJ. New strategies for powder compaction in powder-based rapid prototyping techniques. Procedia CIRP 2013;6:527–32.
[92] Niino T, Sato K. Effect of powder compaction in plastic laser sintering fabrication. In: Proceedings of the 20th Annual International Solid Freeform Fabrication Symposium; 2009 Aug 3–5; Austin, TX, USA; 2009. p. 193–205.
[93] Haferkamp H, Ostendorf A, Becker H, Czerner S, Stippler P. Combination of Yb:YAG-disc laser and roll-based powder deposition for the micro-laser sintering. J Mater Process Technol 2004;149(1–3):623–6.
[94] Gibson I, Rosen D, Stucker B. Additive manufacturing technologies: 3D printing, rapid prototyping, and direct digital manufacturing. New York: Springer; 2015.
[95] Yang S, Evans JRG. Metering and dispensing of powder; the quest for new solid freeforming techniques. Powder Technol 2007;178(1):56–72.
[96] Matsusaka S, Yamamoto K, Masuda H. Micro-feeding of a fine powder using a vibrating capillary tube. Adv Powder Technol 1996;7(2):141–51.
[97] Matsusaka S, Urakawa M, Masuda H. Micro-feeding of fine powders using a capillary tube with ultrasonic vibration. Adv Powder Technol 1995;6 (4):283–93.
[98] Yang S, Evans JRG. A dry powder jet printer for dispensing and combinatorial research. Powder Technol 2004;142(2–3):219–22.
[99] Li X, Choi H, Yang Y. Micro rapid prototyping system for micro components. Thin Solid Films 2002;420–421:515–23.
[100] Bailey AG. The science and technology of electrostatic powder spraying, transport and coating. J Electrost 1998;45(2):85–120.
[101] Yang Q, Ma Y, Zhu J, Chow K, Shi K. An update on electrostatic powder coating for pharmaceuticals. Particuology 2017;31:1–7.
[102] Fitch CJ, inventor; International Business Machines Corp, assignee. Electrophotographic printing machine. United States patent US2807233A. 1957 Sep 24.
[103] Liew CL, Leong KF, Chua CK, Du Z. Dual material rapid prototyping techniques for the development of biomedical devices. Part 2: Secondary powder deposition. Int J Adv Manuf Technol 2002;19(9):679–87.
[104] Kumar AV, Zhang H. Electrophotographic powder deposition for freeform fabrication. In: Proceedings of the 10th Annual International Solid Freeform Fabrication Symposium; 1999 Aug 9–11; Austin, TX, USA; 1999. p. 647–54.
[105] Kumar AV, Dutta A, Fay JE. Solid freeform fabrication by electrophotographic printing. In: Proceedings of the 14th Annual International Solid Freeform Fabrication Symposium; 2003 Aug 4–6; Austin, TX, USA; 2003. p. 39–49.
[106] Thomas S, Tobias L, Philipp A, Stephan R. Electrostatic multi-material powder deposition for simultaneous laser beam melting. In: International Conference on Information, Communication and Automation Technologies (ICAT); 2014 Aug 14–15; Venice, Italy; 2014.
[107] Melvin III LS, Beaman Jr JJ. A sieve feed system for the selective laser sintering process. In: Proceedings of the 6th Annual International Solid Freeform Fabrication Symposium; 1995 Aug 7–9; Austin, TX, USA; 1995. p. 425–32.
[108] Melvin III LS, Beaman JJ. The electrostatic application of powder for selective laser sintering. In: Proceedings of the 2nd Annual International Solid Freeform Fabrication Symposium; 1991 Aug 12–14; Austin, TX, USA; 1991. p. 171–7.
[109] Swaminathan B, Joshi AM, Patibandla NB, Ng HT, Kumar A, Ng E, et al., inventors; Applied Materials Inc., assignee. Additive manufacturing with electrostatic compaction. United States patent US20160368056A1. 2016 Dec 22.

[110] Paasche N, Brabant T, Streit S, inventors; EOS GmbH Electro Optical Systems, assignee. Layer application device for an electrostatic layer application of a building material in powder form and device and method for manufacturing a three-dimensional object. United States patent US20090017219A1. 2009 Jan 15.
[111] Zhao Y, Koizumi Y, Aoyagi K, Yamanaka K, Chiba A. Characterization of powder bed generation in electron beam additive manufacturing by discrete element method (DEM). Mater Today Proc 2017;4(11):11437–40.
[112] Elliott AM, Nandwana P, Siddel DH, Compton B. A method for measuring powder bed density in binder jet additive manufacturing process and the powder feedstock characteristics influencing the powder bed density. In: Proceedings of the 27th Annual International Solid Freeform Fabrication Symposium; 2016 Aug 8–10; Austin, TX, USA; 2016. p. 1031–7.
[113] Zocca A, Gomes CM, Mühler T, Günster J. Powder-bed stabilization for powder-based additive manufacturing. Adv Mech Eng 2014;6:491581.
[114] Secondary finishing processes in metal additive manufacturing [Internet]. Shrewsbury: Inovar Communications Ltd.; [cited 2018 Jun 30]. Available from: http://www.metal-am.com/introduction-to-metal-additive-manufacturing-and-3d-printing/secondary-finishing-processes/.
[115] Marimuthu S, Triantaphyllou A, Antar M, Wimpenny D, Morton H, Beard M. Laser polishing of selective laser melted components. Int J Mach Tools Manuf 2015;95:97–104.
[116] Spierings AB, Starr TL, Wegener K. Fatigue performance of additive manufactured metallic parts. Rapid Prototyp J 2013;19(2):88–94.
[117] Alrbaey K, Wimpenny DI, Al-Barzinjy AA, Moroz A. Electropolishing of Re-melted SLM stainless steel 316L parts using deep eutectic solvents: 3 × 3 full factorial design. J Mater Eng Perform 2016;25(7):2836–46.
[118] Pyka G, Burakowski A, Kerckhofs G, Moesen M, Van Bael S, Schrooten J, et al. Surface modification of Ti6Al4V open porous structures produced by additive manufacturing. Adv Eng Mater 2012;14(6):363–70.
[119] Mingareev I, Bonhoff T, El-Sherif AF, Meiners W, Kelbassa I, Biermann T, et al. Femtosecond laser post-processing of metal parts produced by laser additive manufacturing. J Laser Appl 2013;25(5):052009.
[120] Lamikiz A, Sánchez JA. López de Lacalle LN, Arana JL. Laser polishing of parts built up by selective laser sintering. Int J Mach Tools Manuf 2007;47(12–13):2040–50.
[121] Ma CP, Guan YC, Zhou W. Laser polishing of additive manufactured Ti alloys. Opt Lasers Eng 2017;93:171–7.
[122] de Wild M, Schumacher R, Mayer K, Schkommodau E, Thoma D, Bredell M, et al. Bone regeneration by the osteoconductivity of porous titanium implants manufactured by selective laser melting: a histological and micro computed tomography study in the rabbit. Tissue Eng Part A 2013;19(23–24):2645–54.
[123] Qu J, Shih AJ, Scattergood RO, Luo J. Abrasive micro-blasting to improve surface integrity of electrical discharge machined WC–Co composite. J Mater Process Technol 2005;166(3):440–8.
[124] Kennedy DM, Vahey J, Hanney D. Micro shot blasting of machine tools for improving surface finish and reducing cutting forces in manufacturing. Mater Des 2005;26(3):203–8.
[125] Wang X, Li S, Fu Y, Gao H. Finishing of additively manufactured metal parts by abrasive flow machining. In: Proceedings of the 27th Annual International Solid Freeform Fabrication Symposium; 2016 Aug 8–10; Austin, TX, USA; 2016. p. 2470–2.
[126] Bagehorn S, Wehr J, Maier HJ. Application of mechanical surface finishing processes for roughness reduction and fatigue improvement of additively manufactured Ti-6Al-4V parts. Int J Fatigue 2017;102:135–42.
[127] Boschetto A, Bottini L, Veniali F. Surface roughness and radiusing of Ti6Al4V selective laser melting-manufactured parts conditioned by barrel finishing. Int J Adv Manuf Technol 2018;94(5–8):2773–90.
[128] Yang L, Gu H, Lassell A. Surface treatment of Ti6Al4V parts made by powder bed fusion additive manufacturing processes using electropolishing. In: Proceedings of the 25th Annual International Solid Freeform Fabrication Symposium; 2014 Aug 4–6; Austin, TX, USA; 2014. p. 268–77.
[129] Yasa E, Kruth JP, Deckers J. Manufacturing by combining selective laser melting and selective laser erosion/laser re-melting. CIRP Ann 2011;60(1):263–6.
[130] Hashimoto F, Yamaguchi H, Krajnik P, Wegener K, Chaudhari R, Hoffmeister HW, et al. Abrasive fine-finishing technology. CIRP Ann 2016;65(2):597–620.
[131] Strickstrock M, Rothe H, Grohmann S, Hildebrand G, Zylla IM, Liefeith K. Influence of surface roughness of dental zirconia implants on their mechanical stability, cell behavior and osseointegration. BioNanoMaterials 2017;18(1–2):20160013.
[132] Klotz UE, Tiberto D, Held F. Additive manufacturing of 18-Karat yellow-gold alloys. In: Proceedings of the 30th Santa Fe Symposium on Jewelry Manufacturing Technology; 2016 May 15–18; Albuquerque, NM, USA; 2016. p. 255–72.
[133] Galimberti G, Doubrovski M, Guagliano M, Previtali B, Verlinden JC. Investigating the links between the process parameters and their influence on the aesthetic evaluation of selective laser melted parts. In: Proceedings of the 27th Annual International Solid Freeform Fabrication Symposium; 2016 Aug 8–10; Austin, TX, USA; 2016. p. 2367–86.
[134] Liu C, Liu Z, Wang B. Modification of surface morphology to enhance tribological properties for CVD coated cutting tools through wet micro-blasting post-process. Ceram Int 2018;44(3):3430–9.
[135] Tan KL, Yeo SH. Surface modification of additive manufactured components by ultrasonic cavitation abrasive finishing. Wear 2017;378–379:90–5.
[136] Guo J, Kum CW, Au KH, Tan ZE, Wu H, Liu K. New vibration-assisted magnetic abrasive polishing (VAMAP) method for microstructured surface finishing. Opt Express 2016;24(12):13542–54.
[137] Delfs P, Li Z, Schmid HJ. Mass finishing of laser sintered parts. In: Proceedings of the 26th Annual International Solid Freeform Fabrication Symposium; 2015 Aug 10–12; Austin, TX, USA; 2015. p. 514–26.
[138] Javier Gil F, Planell JA, Padrós A, Aparicio C. The effect of shot blasting and heat treatment on the fatigue behavior of titanium for dental implant applications. Dent Mater 2007;23(4):486–91.
[139] Grubova I, Priamushko T, Surmeneva M, Korneva O, Epple M, Prymak O, et al. Sand-blasting treatment as a way to improve the adhesion strength of hydroxyapatite coating on titanium implant. J Phys Conf Ser 2017;830:012109.
[140] Felix C. Surface treatment for medical parts [Internet]. Cincinnati: Gardner Business Media Inc.; c2019 [updated 2007 Jul 16; cited 2018 Jun 30]. Available from: https://www.productionmachining.com/articles/surface-treatment-for-medical-parts(1).
[141] Lorenz KA, Jones JB, Wimpenny DI, Jackson MR. A review of hybrid manufacturing. In: Proceedings of the 27th Annual International Solid Freeform Fabrication Symposium; 2015 Aug 10–12; Austin, TX, USA; 2015. p. 96–108.
[142] Lauwers B, Klocke F, Klink A, Tekkaya AE, Neugebauer R, Mcintosh D. Hybrid processes in manufacturing. CIRP Ann 2014;63(2):561–83.
[143] Nagel JKS, Liou FW. Hybrid manufacturing system modeling and development. In: Proceedings of the ASME 2012 International Design Engineering Technical Conferences and Computers and Information in Engineering Conference; 2012 Aug 12–15; Chicago, IL, USA. New York: The American Society of Mechanical Engineers; 2012. p. 189–98.
[144] Flynn JM, Shokrani A, Newman ST, Dhokia V. Hybrid additive and subtractive machine tools—research and industrial developments. Int J Mach Tools Manuf 2016;101:79–101.
[145] Whitesides GM. The origins and the future of microfluidics. Nature 2006;442(7101):368–73.
[146] Amin R, Knowlton S, Hart A, Yenilmez B, Ghaderinezhad F, Katebifar S, et al. 3D-printed microfluidic devices. Biofabrication 2016;8(2):022001.
[147] Steigert J, Haeberle S, Brenner T, Müller C, Steinert CP, Koltay P, et al. Rapid prototyping of microfluidic chips in COC. J Micromech Microeng 2007;17(2):333–41.
[148] Ho CM, Ng SH, Li KH, Yoon YJ. 3D printed microfluidics for biological applications. Lab Chip 2015;15(18):3627–37.
[149] Shiu PP, Knopf GK, Ostojic M, Nikumb S. Rapid fabrication of micromolds for polymeric microfluidic devices. In: Proceedings of the 2007 Canadian Conference on Electrical and Computer Engineering; 2007 Apr 22–26; Vancouver, BC, Canada. New York: IEEE; 2007. p. 8–11.
[150] Shen YK, Lin JD, Hong RH. Analysis of mold insert fabrication for the processing of microfluidic chip. Polym Eng Sci 2009;49(1):104–14.
[151] Becker H, Locascio LE. Polymer microfluidic devices. Talanta 2002;56(2):267–87.
[152] Sawa Y, Yamashita K, Kitadani T, Noda D, Hattori T. Fabrication of high hardness micro mold using double layer nickel electroforming. In: Proceedings of the 2008 International Symposium on Micro-Nano Mechatronics and Human Science; 2008 Nov 6–9; Nagoya, Japan. New York: IEEE; 2008. p. 402–7.
[153] Zhang N, Srivastava AP, Browne DJ, Gilchrist MD. Performance of nickel and bulk metallic glass as tool inserts for the microinjection molding of polymeric microfluidic devices. J Mater Process Technol 2016;231:288–300.
[154] Kim K, Park S, Lee JB, Manohara H, Desta Y, Murphy M, et al. Rapid replication of polymeric and metallic high aspect ratio microstructures using PDMS and LIGA technology. Microsyst Technol 2002;9(1–2):5–10.
[155] GE Additive. How additive is helping innovators transform dental implantology [Internet] General Electric.; c2019 [cited 2019 Apr 13] Available from: https://www.ge.com/additive/case-studies/how-additive-helping-innovators-transform-dent-al-implantology.
[156] 3D Systems. Direct metal 3D printing brings growth benefits to MicroDent dental lab [Internet]. Valencia: 3D Systems, Inc.; c2019 [cited 2018 Jun 30]. Available from: https://www.3dsystems.com/learning-center/case-studies/direct-metal-3d-printing-brings-growth-benefits-microdent-dental-lab.
[157] Nyce AC. An assessment of the 2026 U.S. markets and technology for jewelry manufactured by 3D-precious metal printing (3D-PMP) of gold, platinum, and palladium powders [Internet]. Birmingham: Cookson Precious Metals Ltd.; c2015 [cited 2018 Jun 30]. Available from: https://www.cooksongold-emanufacturing.com/img/downloads/3DPMP_Jewelry_markets_2026.pdf.
[158] Zito D, Allodi V, Sbornicchia P, Rappo S. Why should we direct 3D print jewelry? A comparison between two thoughts: today and tomorrow. In: Proceedings of the 31th Santa Fe Symposium on Jewelry Manufacturing Technology; 2017 May 21–24; Albuquerque, NM, USA; 2017. p. 515–56.
[159] Pogliani C, Alberto A. Case study of problems and their solutions for making quality jewelry using selective laser melting (SLM) technology. In: Proceedings of the 30th Santa Fe Symposium on Jewelry Manufacturing Technology; 2016 May 15–18; Albuquerque, NM, USA; 2016. p. 431–58.